



UNIVERSIDADE DA BEIRA INTERIOR
Ciências da Saúde

Is there a Role for Sweet Taste Receptors in the Warburg Effect, Angiogenesis and Cell Survival in Glioblastoma?

Inês da Silva Tavares da Cruz

Dissertação para obtenção do Grau de Mestre em
Ciências Biomédicas
(2º ciclo de estudos)

Orientador: Prof.^a Doutora Cecília Reis Alves Santos
Co-orientador: Prof.^a Doutora Isabel Maria Theriaga Mendes Varanda
Gonçalves

Covilhã, junho de 2019

Acknowledgements

This work would not have been possible without the contribution and help of many people and entities, to which I have to thank.

Firstly, I would like to thank PhD Professor Cecília Santos for giving me the opportunity of working in my field of interest, with which I was able to learn and grow immensely. I thank for the guidance and motivation throughout this year.

A big thanks to the rest of the research group, namely PhD Professor and my co-supervisor Isabel Gonçalves, PhD Telma Quintela and all PhD students Ana Catarina Duarte, Raquel Brito, Daniela Talhada, Joana Tomás and Duarte Rocha, for providing a supportive environment with which I learned every day. A very special thanks to PhD student Ana Raquel Costa, who guided me through every step of the way, transmitted essential knowledge and advice and was the essential help through immense adversities. I would also like to thank PhD Professor José F. Cascalheira and PhD Helena Marcelino, who made the effort of providing me with resources for my work, without which it would not have been possible.

To all of the dear friends, such as João, Beatriz, Augusto and Leandro, who made the toughest days much brighter. They have made me feel welcome, understood and always had a helping hand to offer. A very special thanks to Mariana Oliveira, my lab colleague, classmate and overall true friend who has been through the entire process along with me.

To my boyfriend, Denis, who has gone beyond his capabilities to help me through the most difficult times and to always encourage me to be better, not give up and lose faith in myself.

To my parents for providing me with this wonderful opportunity to grow and have a purposeful life. For being role models and my biggest supporters. And to my grandfather Carlos, his pride and faith in me will never be forgotten and will always push me to be the best professional and overall person I can be.

This study was supported by funding projects such as ICON - Interdisciplinary Challenges On Neurodegeneration (CENTRO-01-0145-FEDER-000013), CENTRO 2020 and Lisboa 2020 (POCI-01-0145-FEDER-016822).

Resumo Alargado

Glioblastoma Multiforme (GBM) é um tipo de tumor cerebral primário de origem astrocitária de grande agressividade e com mau prognóstico, pois doentes possuem uma esperança média de vida de 14 a 15 meses após o diagnóstico. Devido à sua alta complexidade, heterogeneidade e grande capacidade de quimioresistência, a procura de uma melhor compreensão dos mecanismos presentes nas células de GBM que permitem a progressão do tumor torna-se um assunto de elevada importância. GBM, como a maioria das células tumorais, possui um metabolismo alterado, tendo dominância a glicólise, mesmo em situações de concentrações elevadas de oxigénio. A esta reprogramação chama-se o Efeito de Warburg.

Recetores de Sabor Doce (STR), heterodímeros com as subunidades T1R2 e T1R3, são recetores comumente associados à cavidade oral, com a função de reconhecer moléculas doces e despoletar a percepção do sabor doce. No entanto, na última década, têm sido encontrados em diversos órgãos e tecidos. Não só estão presentes ao longo de todo o tracto gastrointestinal, como o epitélio nasal, testículos, espermatozóides, e em locais do SNC como o hipotálamo e tronco cerebral. Há indícios ainda de que os STR têm um papel importante como sensores de glucose em astrócitos e neurónios, aspeto essencial para o seu metabolismo.

Assim, levantou-se a hipótese de que as células de GBM não só possuem estes receptores, como também dependem destes para a manutenção da homeostase do seu metabolismo, contribuindo para a sua sobrevivência, ao serem capazes de detectar glucose. Realizou-se RT-PCR para analisar a presença de transcritos das subunidades T1R2 e T1R3 nas linhas celulares GBM U-87MG, SNB19 e U-373MG, assim como em astrócitos humanos normais (HA). Além disso, foi também analisada a expressão proteica, por Imunocitoquímica e Western Blot, das subunidades do STR e de GLUT1, um importante transportador de glucose em GBM, nas mesmas linhas celulares. Testes de Viabilidade Celular, realizados com múltiplas concentrações de glucose, com e sem inibição do receptor com lactisole, revelaram um notável efeito negativo da sobrevivência das células de SNB19 aquando da inibição do recetor. Realizaram-se ensaios de migração para verificar o efeito das mesmas condições dos ensaios de viabilidade na proliferação e migração celular. Observou-se um efeito negativo da inibição do recetor em SNB19, visto que a migração não era tão eficaz com exposição a lactisole. Os resultados poderão indicar importância dos recetores presentes em GBM no funcionamento normal do seu metabolismo, embora fosse necessária investigação mais aprofundada acerca de outros aspetos em que STRs possam ter efeito no metabolismo de células de GBM, como o efeito de Warburg, através da avaliação celular do lactato, mas também avaliação do efeito dos STRs na angiogénese induzida por hipóxia.

Palavras-chave

Recetores de Sabor Doce, Glioblastoma, Metabolismo de Glucose

Abstract

Glioblastoma (GBM) is a type of primary brain tumour of astrocytic origin with very poor prognosis. Most patients with GBM have an average life expectancy of 14 to 15 months after diagnosis. Due to GBM's high complexity, heterogeneous biology and high level of chemoresistance, different approaches to therapy need to be traced.

Recently, it has been discovered that Sweet Taste Receptors (STRs), usually known as receptors that sense glucose and other sweet molecules allowing sweet taste perception to be triggered in the mouth, can be found in a variety of other organs and tissues. Not only has the STR been found along the entire Gastrointestinal tract, as it has also been located in the nasal epithelium, sperm, testes and some Central Nervous System areas such as the hypothalamus, brainstem and in the choroid plexus. Other findings suggest that STRs may play an important role in neuronal and astrocyte glucose sensing, which is an essential function for their metabolism.

It was hypothesized that STRs were present in GBM cells and would play an important role in their metabolic homeostasis and ultimate survival and proliferation. To test the expression of STRs on GBM cell lines, conventional RT-PCR was done in U-87MG, SNB19 and U-373MG and normal human astrocytes (HA) cells and indicated the presence of transcripts of both subunits T1R2 and T1R3, on GBM cell lines, but not in HA, as only T1R2 was sequenced. Furthermore, using Western Blot and Immunocytochemistry, we have detected protein expression of STR subunits, as well as having confirmed the prominent appearance of GLUT1 in these cells. The role of STRs on cell survival and proliferation was tested by inhibiting them with lactisole in cell viability and migration assays. Results of the mentioned assays lead to the conclusion that not only are STRs present in GBM cell lines, but they certainly have a positive effect in maintaining cell survival and proliferation in the SNB19 cell line, while in U-373MG their role does not seem to be as significant. Further tests need to be done on STR impact on GBM cells Warburg effect through the measurement of lactate release with activation or inhibition of the receptor, as well as on hypoxia induced angiogenesis, when in conditions of oxygen deprivation.

Keywords

Sweet Taste Receptors, Glioblastoma, Glucose Metabolism

Index

Introduction	1
1. Glioblastoma	2
1.1 Glioblastoma Chemoresistance	2
2. Glucose Metabolism in Cancer	3
3. Sweet Taste Receptors and Glucose Metabolism	6
3.1 Activation of the Sweet Taste Receptors	8
3.2 Ectopic Expression of Sweet Taste Receptors	8
Aims	13
Materials and Methods	15
1. Glioblastoma Cell Lines	16
1.1 Cell Culture	16
1.2 Cell Passage	16
1.3 Cell Counting	17
1.4 Cell Freezing and Thawing	17
2. Total RNA	17
2.1 Extraction	18
2.2 Determination and quantification of total RNA integrity	18
2.3 DNase I Treatment	18
3. cDNA synthesis	19
4. Reverse-transcriptase PCR	19
5. Western Blot	20
6. Immunocytochemistry	21
7. Migration Assay	21
8. Cell Viability Assay	22
9. Statistical Analysis	22
Results	23
1. Reverse Transcriptase PCR	24
2. Western Blot	26
3. Immunocytochemistry	27
4. Cell Viability Assay	29
5. Migration Assay	33
Discussion and Conclusion	45
Bibliography	49

Figures List

Figure 1 - Oxidative phosphorylation and anaerobic glycolysis *versus* aerobic glycolysis (the Warburg Effect).

Figure 2 - Structure of the Sweet Taste Receptor.

Figure 3 - T1R2 and T1R3 immunohistochemistry on mouse Choroid Plexus .

Figure 4 - Gel electrophoresis of RT-PCR products of both T1R2 and T1R3 in GBM cell lines and normal human astrocytes.

Figure 5 - Western blot of protein extracts of GBM cell lines and HA.

Figure 6 - Western blot quantification of T1R2 protein expression in GBM cells and HA.

Figure 7 - Representative images for the expression of T1R2 and T1R3 in GBM cell lines U-87MG, SNB19 and U-373MG.

Figure 8 - Representative images for the expression of GLUT1 in GBM cell lines U-87MG, SNB19 and U-373MG.

Figure 9 - Cell viability assay results for SNB19 cells at different glucose concentrations for 24, 48 and 72 hours, in the presence or absence of lactisole.

Figure 10 - Cell viability assay results for U-373MG cells at different glucose concentrations for 24, 48 and 72 hours, in the presence or absence of lactisole.

Figure 11 - SNB19 migration assay representative images at 0, 24, 48 and 72 hours after incubation with different glucose concentrations, in the presence or absence of lactisole.

Figure 12 - Migration rate of SNB19 cells at 24, 48 and 72 hours after incubation with different glucose concentrations, in the presence or absence of lactisole

Figure 13 - Overall migration rate of SNB19 cells at 24 (●), 48 (■) and 72 (▲) hours after incubation with different glucose concentrations.

Figure 14 - U-373MG migration assay representative images at 0, 24, and 48 hours after incubation with different glucose concentrations, in the presence or absence of lactisole.

Figure 15 - Migration rate of U-373MG cells at 24 and 48 hours after incubation with different glucose concentrations, in the presence or absence of lactisole.

Figure 16 - Overall migration rate of U-373MG cells at 24 (●) and 48 (■) hours after incubation with different glucose concentrations.

Tables List

Table 1 - Sweet Taste Receptors found in ectopic areas and their function.

Table 2 - T1R2 and T1R3 Forward and Reverse primers.

Table 3 - Homology percentage of T1R2 and T1R3 in all GBM cell lines and HA, when compared to *Homo Sapiens* sequence database (NCBI-Blast).

Acronyms List

ATD	Amino Terminal Domains
CRD	Cysteine Rich Domain
DEPC	diethylpyrocarbonate
DMEM	Dulbecco's Modified Eagle Medium
DMSO	Dimethyl Sulfoxide
ECM	Extracellular Matrix
FBS	Fetal Bovine Serum
GBM	Glioblastoma Multiforme
GLUT1	Glucose Transporter 1
GPCR	G-Protein Coupled Receptor
GSC	Glioblastoma Stem Cell
HIF1	Hypoxia-inducible Factor 1
mGluR	Metabotropic Glutamate Receptor
MTIC	5-3-(methyl)-1-(triazene-1-yl)imidazole-4-carboxamide
MTT	3-(4,5-dimethylthiazol-2-yl)-2,5-diphenyltetrazolium bromide
PBS	Phosphate Buffered Saline
PBS-T	Phosphate Buffered Saline with Tween-20
PLC β 2	Phospholipase C β 2
RT-PCR	Reverse-Transcriptase Polymerase Chain Reaction
STR	Sweet Taste Receptor
T1R	Taste 1 Receptor Family
T1R1	Taste 1 Receptor Family Member 1
T1R2	Taste 1 Receptor Family Member 2
T1R3	Taste 1 Receptor Family Member 3
T2R	Taste 2 Receptor Family
TBS	Tris-buffered saline
TBS-T	Tris-buffered saline with Tween-20
TMD	Transmembrane Domains
TME	Tumour Microenvironment
TMZ	Temozolomide

Introduction

1. Glioblastoma

Glioma is the name given to a primary brain tumour derived from glial cells which can be classified according to their suspected cellular origin. Among these are Glioblastoma Multiforme (GBM), a tumour of astrocytic origin and the most malignant and frequently occurring type of all primary astrocytomas. In fact, the World Health Organization designated GBM as the most aggressive, invasive and undifferentiated type of tumour, classifying it as a Grade IV tumour, the highest in parameters of invasiveness and malignancy [1]. GBM is most frequently found in the cerebral hemispheres since 95% of tumours are found in the supratentorial region and only a few cases occur in regions like the cerebellum, brainstem or spinal cord.

Patients with GBM have a median survival of 14 to 15 months after diagnosis [2]. The tumour can appear at any age, but the peak occurs in patients with 55 to 60 years old. It is more incident in men than in women [3] and also most frequently reported in developed countries [4]. A few studies revealed that GBM development seems to be influenced by ovarian steroid hormones[5]. Also, infection and allergic diseases may have a protective effect on GBM, possibly due to the activation of the immune surveillance mechanism [6].

So far, there are no carcinogenic causes identified for these tumours. The only confirmed risk is the exposure to a high dose to ionizing radiation, but there is no confirmed association between GBM and environmental factors such as smoking, dietary risk factors, electromagnetic field, occupational risk factors, head injury or pesticide exposure. Moreover, although gliomas seem to run in families, a susceptibility gene has not been identified yet [4].

Currently, the standard treatment procedure is therapeutic management, which usually includes surgical resection of the tumour along with radiation and temozolomide therapy, and also with symptomatic relief treatments of neurological symptoms that can be associated with the tumour [4].

1.1 Glioblastoma Chemoresistance

Because of its high complexity and heterogeneous biology, there are many challenges to treating GBM. However, GBM malignancy, invasiveness and therapy failure are also due to its excellent capacity to interact with its microenvironment [7]. The tumour microenvironment (TME) harbours different types of cells, such as stromal, endothelial and immune cells, along with the extracellular matrix (ECM), with cytokines, growth factors and conditions such as hypoxia and acidosis. The TME interacts with glioblastoma stem cells (GSCs) and support their biological mechanisms that will ensure tumour progression and therapeutic resistance [8]. Specifically, unresponsiveness to therapy can be promoted through altered expression of multidrug resistance genes present in GBM heterogeneous group of cells [9]. It is also

immunosuppressive, as cancer can sidestep immune surveillance [10]. Also, the blood-brain barrier with its poor permeability will have a role in therapy resistance, as it will not allow for most attempts of therapy to contact with tumour tissue [11].

Nitrosoureas such as nimustine, carmustine and lomustine have been used for decades, having now been replaced with the current medication of choice, temozolomide (TMZ). TMZ has a rapid non-enzymatic conversion at physiologic pH to its reactive compound 5-(3-methyl-1H-imidazo[4,5-f]pyridin-2-yl)-1H-imidazole-4-carboxamide (MTIC). One of the MTIC mechanisms of action relies on damaging the tumour DNA by methylating the O⁶ position of guanine, which will cause it to mismatch with thymine. Recurrent G-T mismatches will further cause double-stranded DNA breaks, critical recombinogenic secondary lesions and further aberrations [12].

It is important to mention that tumours are thought to be driven by subpopulations of tumour cells with stem cell-like properties, called Cancer Stem Cells (CSCs). They proliferate as progenitor-like and can survive upon intensive oncological therapies, which allows them to trigger tumour recurrences. Therapies that will focus on eliminating the tumour portion of CSCs are, therefore, more capable of inducing long term responses and thereby halt tumour progression. However, therapies which will exclusively target CSCs may not result in significant shrinkage of the tumour, as it will only prevent tumour proliferation, resulting in a persisting period of a stable tumour [12].

2. Glucose Metabolism in Cancer

Cellular metabolism in a solid tumour is different from that of the normal tissue. In cancer cells, there is a more frequent use of the glycolytic process for energy acquirement, instead of the more frequent usage of oxidative phosphorylation in normal cells. Glycolysis is a process that transforms glucose into pyruvate, with the production of two molecules of ATP. This low-yield energy production is enough to supply ATP for cellular energetics if the supply of glucose is adequate [13]. Oxidative phosphorylation is another form of energy production, where oxygen is used as an electron acceptor from intermediate compounds that arise from the transformation of glucose. This process can produce ATP with a higher yield, up to 36 molecules of ATP per one molecule of glucose. Bearing this in mind, it is reasonable to question why cancer cells prefer to use glycolysis as their main source of energy, as observed by Otto Warburg [14].

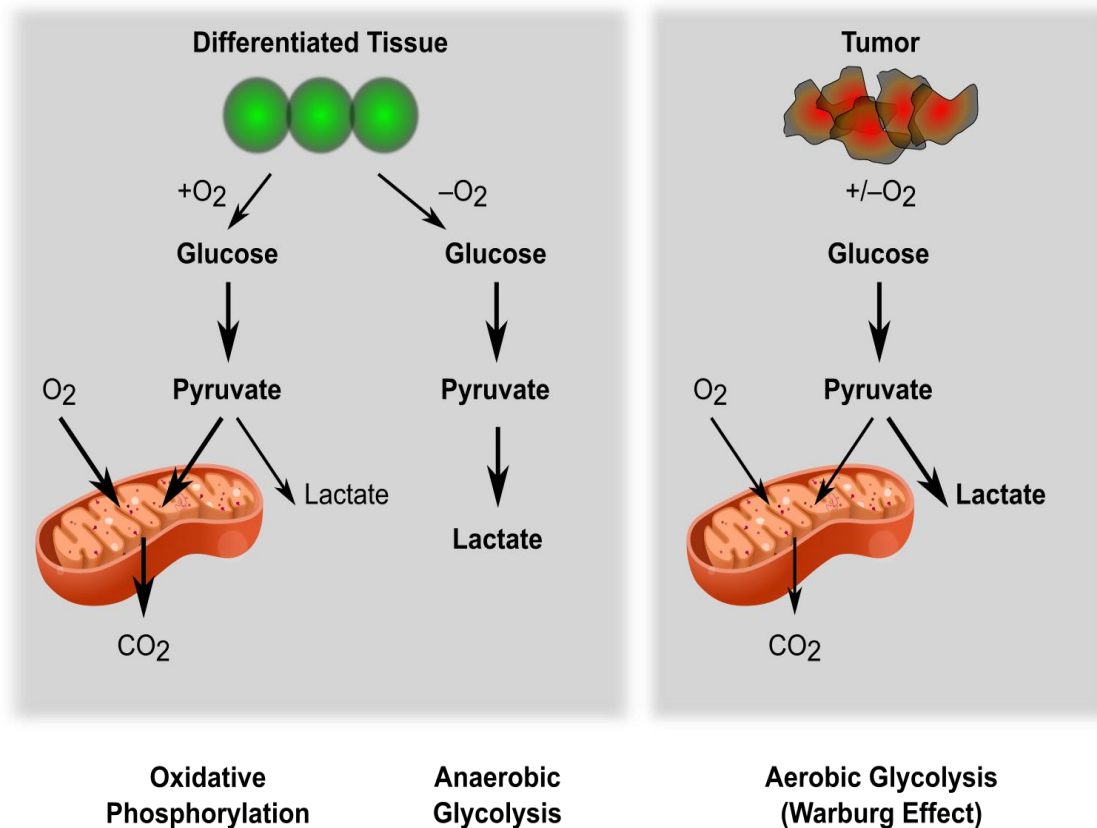


Figure 1 - Oxidative phosphorylation and anaerobic glycolysis versus aerobic glycolysis (the Warburg Effect). Tumour cells will tend to use glycolysis as the main source of energy, even in the presence of oxygen, contrarily to normal cells, which will preferably use oxidative phosphorylation in favourable conditions (adapted from [15]).

One of the possible explanations resides in the characteristics of tumour environment. Within a tumour, we can find conditions like acidosis, higher pressure of interstitial fluid and hypoxia, and all of them are sources of stress due to the deficient vascularization caused by the poor ability of angiogenesis by the tumorous tissue. Hypoxia is particularly important for metabolic changes in tumour cells, since it allows the activation of the hypoxia-inducible factor 1 (HIF1), which will stimulate the production of glycolytic energy by transactivating genes that translate into molecules involved in the transport of extracellular glucose. HIF1 is constituted by two subunits: HIF1 β is constitutively expressed, whereas HIF1 α has a short half-life and its expression depends greatly on the available level of oxygen. More than 100 genes have been identified to target HIF1 α and, when expressed, it can form a heterodimer with HIF1 β and promote angiogenesis, cell survival, boost glucose metabolism and tumour invasion [16]. The activation of HIF1 and the HIF1 transcriptional programme have two main effects on metabolism that serve to balance O₂ consumption with O₂ supply. The first main effect is that HIF1 stimulates glycolytic energy production by transactivating genes involved in extracellular glucose import, such as glucose transporter 1 (GLUT1), also known as solute carrier family 2 member 1, and enzymes responsible for the glycolytic breakdown of intracellular glucose, such

as phosphofructokinase 1 and aldolase. HIF1 contributes for glycolysis by activating the production of enzymes that are responsible for the glucose breakdown in the glycolytic process. HIF1 will also directly inhibit oxidative phosphorylation, once glycolysis might not be as efficient as an energy production source, but it will do so without the need of oxygen, which is an essential feature for tumour cells to have in their specific hypoxic environment [17].

In glioblastoma multiforme, there is characteristically a high degree hypoxia, since the pressure of oxygen inside the tumour can drop to as low as 1%. However, GBM cells have methods to resist hypoxia and, consequently, become more aggressive. For example, autophagy, a catabolic process, can be one of the ways cells find to be protected from stress in a hypoxic environment. This process is characterized by the degradation of various cell components for an alternative method of production of ATP [16]. Hypoxic areas are formed by an uncontrolled proliferation of cancer cells, which will lead to a dense and unorganized tissue. The tumour will have the need to form new vessels, and for this, HIF1 will promote the release of vascular endothelial growth factor, thus promoting angiogenesis. Nonetheless, angiogenesis can still lead to hypoxia, as neovascularization can result in abnormal, small and occluded vessels, that bring an insufficient supply of oxygen, which will maintain the condition of hypoxia. Cells will need to find a different method to overcome the hypoxic stress, so they become more aggressive, even more resistant to possible cancer treatments [16].

Hypoxia cannot fully explain the Warburg effect, however, because cancer cells can also utilize glycolysis as the main source of energy even in a facilitated exposure to oxygen [14]. For example, leukemic cells have a high level of oxygen exposure due to circulation within the bloodstream. Still, leukemic cells have shown to have a high use of glycolysis. Thus, although hypoxia is an important aspect to consider in the understanding of cancer biology, evidences suggest that it is not the only major contributor to the metabolic switch in cancer cells [17].

Proliferating cells are in a major need of resources that will enable them to replicate all of the cellular contents during the cell cycle. There is a large requirement of nucleotides, amino acids and lipids. In this instance, glucose is not only used for ATP production, but also for generating biomass. As an example, it is known that the production of amino acids and nucleotides can consume more equivalents of carbon and NADPH than of ATP. It is clear by this that glucose cannot be exclusively committed to produce ATP in a proliferating cell as a cancer cell, since it would impair the production of intermediates required for macromolecular synthesis, ultimately, impairing growth and proliferation [15].

One of the main particularities in GBM glucose metabolism is its glucose transporters. Glucose uptake is performed by transporters called GLUTs, a family of 14 membrane-bound proteins. In cancer cells, GLUT1 and GLUT3 are the most common. In fact, there is an overexpression of both transporters, especially GLUT1, in response to a hypoxic environment that is directly regulated by HIF1. The glucose transporter most significant overexpression is observed in the

intermediate zone of the tumour. This intermediate region of the tumour is characterized as both moderately hypoxic and exhibiting the highest amounts of HIF1 α within the tumour [18]. On the other hand, GLUT3 is considered the “brain type” glucose transporter, as it is most found in neurons and in brain tumour initiating cells. GLUT3 also appears to perhaps be upregulated in the hypoxic environment, but this is still uncertain. Both GLUT1 and GLUT3 have a high affinity to glucose, which will be an advantage for cancer cells, not only for their own use for cell growth and energy production, but also to deprive the nearest environment from immune cells from glucose, what will compromise their function [19].

An enhanced glucose uptake and its use for glycolysis will translate into a higher concentration of lactic acid. In the case of glioblastoma cells in culture, up to 90% of available glucose is ultimately converted from pyruvate into lactate by the enzyme lactate dehydrogenase A. Most of the produced lactate is secreted as waste to the outside of the cell, in order to remove excess carbon from cytoplasmic environment, and to maintain an ideal NADP⁺ concentration, which will serve as a good source of NADPH production allowing cell growth [15]. On the other hand, more lactic acid within the tumour environment will represent a pH decrease, which leads to a weaker response of the immune cells surrounding the tumour [15].

3. Sweet Taste Receptors and Glucose Metabolism

Humans are capable of distinguishing between five different basic tastes: sweet, salty, umami, bitter and sour. Additionally, lipid sensors have been recently identified on the tongue, which might indicate that fat could be a sixth taste [20]. This ability of taste gives us valuable input: sensing bitter taste triggers aversive behaviours to possibly noxious substances and sensing sweetness will lead to our recognition of high caloric food sources [21]. So far, there have been found four morphologic subtypes of taste receptors cells. Type I corresponds to glial-like cells that can detect the salty taste. Type II cells have G-protein coupled receptors (GPCRs) and thus can detect sweet, umami and bitter tastes. Type III cells can detect sourness, whereas Type IV corresponds to stem or progenitor taste cells [22].

Concerning the type II cells, there have been found two different classes of GPCRs: taste 1 receptor family (T1R) and taste 2 receptor family (T2R). The T1R family proteins are linked to the sweet and umami tastes and belong to the glutamate family which include the members 1 (T1R1), 2 (T1R2) and 3 (T1R3) in humans and mammalian species. Among these, T1R2 and T1R3 form heterodimers to serve as sweet taste receptors (STRs) [23], [24]. Both T1R2 and T1R3 belong to a subclass of GPCRs that resemble the metabotropic glutamate receptor (mGluR), the calcium-sensing receptor and pheromone receptors [25]. Like all GPCRs, STRs are constituted by amino terminal domains (ATD) and transmembrane domains (TMD) [26]. The ATD

contain a Venus flytrap domain and a short cysteine rich domain (CRD), and this last domain is the connection between ATD and the α -helical TMD, which is also characteristic of GPCRs [27].

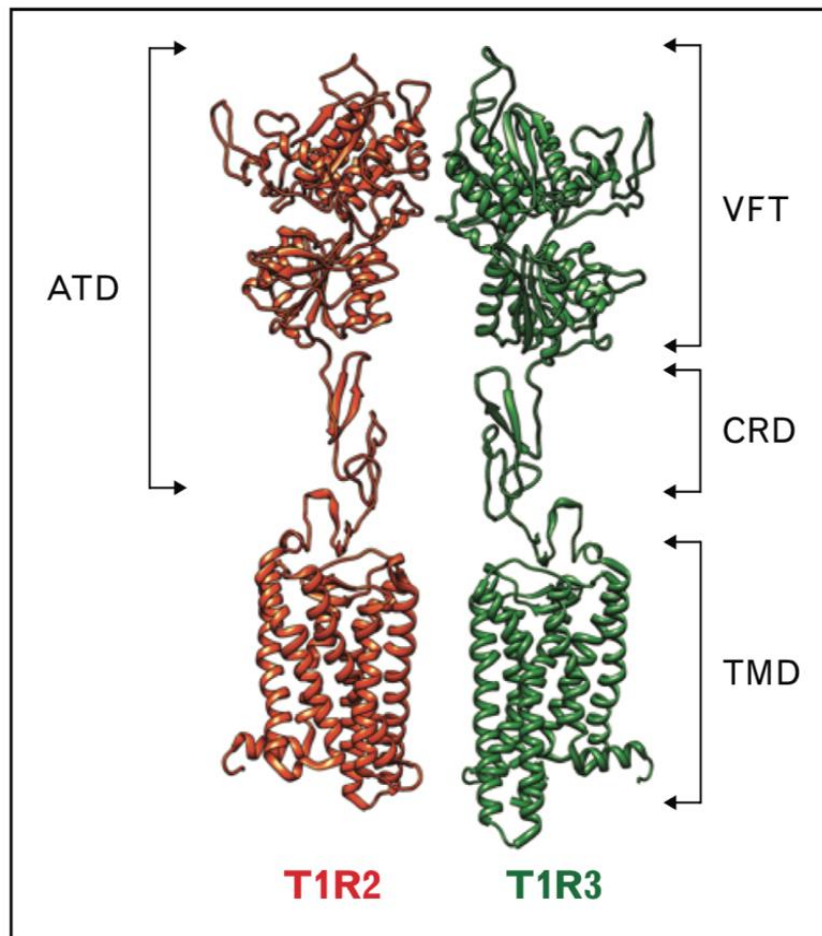


Figure 2 - Structure of the Sweet Taste Receptor, containing T1R2 and T1R3, each with an aminoterminal domain (ATD), which includes a Venus Flytrap domain (VFT) and Cysteine Rich domain (CRD), and a Transmembrane domain (TMD) (adapted from [27]).

Based on the structure similarity between sweet taste receptors and mGluR1, the binding of ligands is seen as a way to stabilize the active form of the STRs by binding them within the cleft [25]. There is, at least, four different ligand-binding domains in the STRs subunits, which might explain the ability of the receptor to be activated by structurally different several compounds with different magnitude of affinity [28]. Sweet taste receptors can, indeed, be activated by a wide range of chemically different compounds, such as sugars (glucose, maltose, sucrose and fructose), artificial sweeteners (saccharin, aspartame, cyclamate), sweet amino acids (D-tryptophan, D-phenylalanine, D serine) and sweet proteins (monellin, brazzein, thaumatin) [20]. Additionally, T1R3 has shown the ability to form a homodimer that is sensitive to monosaccharides and disaccharides, but only when these compounds are at high concentrations [29]. These agonists can either activate the receptor by stabilizing the closed conformations of the VFD of the T1R2 subunit, or by interacting with either of both TMDs of the receptor.

Additional residues located in the CRD of T1R3 hold some importance for the receptor activation by sweet proteins [28]. It is known that the TMD of T1R2 interacts functionally with the G protein, but it is not yet clear how signaling occurs from the VFD of T1R2 or even from the TMD or the CRD of T1R3 [28].

Some studies in mice show a specific gene region that modulates the response to many sweet compounds. This locus is called Sac. While testing the possible connection of Sac with genes that encode the known STRs, genetic mapping was performed, and it was found that two of the T1Rs— T1R1 and T1R2 – were located in the distal end of chromosome 4 but are separated from the Sac locus. Nonetheless, T1R3 was shown to be tightly associated with Sac [21]. Within the chromosome, they are disposed in the order: Tas1r2–Tas1r1–Tas1r3 [30]. However, the same was not observed in humans, since there are significant genetic variations concerning the sweet taste among different species. The three human TAS1R genes are located in the short arm of human chromosome 1 (1p36) in the following order: TAS1R2– TAS1R1–TAS1R3 [30].

3.1 Activation of the STR

The sweet taste can be sensed by a process that starts with the recognition of one of the many ligands that STRs bind to, as mentioned above. The number of receptors associated with sweet taste is modest, compared to the number of bitter taste receptors [21]. Interestingly, taste cells that detect bitterness will respond to a wide array of compounds but will not be able to discriminate them. The sweet taste system, on the other hand, can recognize and distinguish a variety of pathways associated with the recognition of the different sweet tastes [21].

All type II taste cell have a similar signaling cascade. Once the ligand binds to the receptor, a signaling chain of events happen, resulting on the depolarization of the cell. The heterotrimeric G-protein α -gustducin, phospholipase C β 2 (PLC β 2), inositol-3-phosphate receptors and transient receptor potential channel M5 (TRPM5) are all found in taste cells and all have a role on the signaling cascade [31]. The binding of a ligand to the sweet taste receptor leads to the activation of α -gustducin. Consequently, PLC β 2 is stimulated, which triggers the inositol trisphosphate-mediated release of calcium and, therefore, activates TRPM5. This sequence of events results in the release of ATP, which will then activate the adjacent sensory afferent neurons and lead to taste perception by sending signals to the appropriate brain centers [32].

3.2 Ectopic Expression of Sweet Taste Receptors

Like all taste receptors, sweet taste receptors are commonly known to be located in the mouth, especially in the tongue. However, recent studies have found that STRs are expressed throughout the body, including the nasal epithelium, the respiratory system, in the pancreatic islet cells, sperm, testes and in the gastrointestinal tract [20].

Pancreatic β -cells are a particular set of cells that are important to mention. The sweet taste receptor expressed in the pancreatic β -cells is unique in the way that it activates both calcium and cAMP messenger systems. Since agents that increase cAMP production in the cells will protect them from stress and apoptosis, the sweet taste receptor may be a potential target for therapy to treat metabolic diseases such as diabetes [33]. These findings were also corroborated by studies in the gut of rat and swine models, where an increase of incretin release after the binding of non-nutritive sweeteners to STRs was observed [34]. As incretins are important hormones for the regulation of glucose in the bloodstream, this study may highlight the relevance of STRs in the understanding and treatment of obesity and type 2 diabetes.

Evidences shown that STRs located in L-cells, pancreatic β -cells and other cells along the gastrointestinal tract will modulate insulin release by recognizing sweet compounds like fructose and glucose, thus contributing to glucose metabolism and hormone secretion [35]; [36]; [37].

Besides the gastrointestinal tract and central nervous system, STRs have been found in mice nasal solitary chemosensory cells and in human sinonasal tissues, indicating that there is a response to molecules that are secreted by respiratory pathogens, suggesting that STRs may influence immune responses and pathogen clearance [38][39], [40]. Studies in mice also show that their myogenesis may be affected by STRs. MyoD and myogenin, important molecules for muscle development and differentiation, upregulate T1R3, consequently affecting muscle cell proliferation and organ homeostasis [34]. All of these examples indicate the importance of sweet taste receptors on cell proliferation, homeostasis and capacity of response to specific stimuli and are described with more detail in the table below.

Table 1 - Sweet Taste Receptors found in ectopic areas and their function.

Organism / Cells	Disease/ Circumstance	Ligands / Signaling	Functions	References
Mouse: nasal solitary chemosensory cells; Human: tissue from Sino nasal locations;	Chronic Rhinosinusitis; Sino nasal infection;	STRs respond to quorum-sensing molecules called acyl-homoserine lactones that are secreted by respiratory pathogens;	Genetic variation of STRs correlates with different sweet taste preferences in humans and may also explain different immune responses and pathogen clearance;	[38], [39], [40]
Gut (mice and swine models);	Treatment of Obesity and type 2 Diabetes;	Non-nutritive sweeteners (NNS);	Incretin release in response to the NNS binding;	[34]
Muscle Cells (mice)	myogenesis	MyoD and myogenin;	MyoD and myogenin: upregulation of T1R3 expression, affecting muscle cell proliferation	[34]

			and organ homeostasis;	
Mice with helminth infection: tuft/brush cells;	parasitic infection;	--	STRs sense parasites, triggering the release of IL-25, which increases proliferation of tuft cells and initiates type II immune response;	[34]
Human Gastric Parietal Tumor Cells	--	Artificial Noncaloric Sweeteners (NCS): cyclamate, acesulfame potassium, sucralose, saccharin, neohesperidin dihydrochalcone	synthesis and release of 5-HT upon stimulation with NCS;	[41]
Human and mouse islets, MIN6 cells, pancreatic beta cells;	--	Fructose, sucrose;	T1R2 is responsible for fructose-induced insulin release; T1R3 stimulates glucose-stimulated insulin secretion through rapid increasing of cytoplasmic calcium and cAMP;	[35]
L cells (gut) in rats;	Type 2 diabetes;	Glucose;	STR expression is associated with altered glucose metabolism;	[36]
Human (gastrointestinal tract): healthy lean participants;		Saccharin as stimulant and lactisole as inhibitor;	Inhibition of STRs with lactisole will alter insulin response;	[37]
Mice	Obesity	--	Expression in the hypothalamus and brainstem of STRs differ in obesity; Hypothalamus and brainstem are key locations for metabolic modulation;	[42]
Rat hippocampus	Transient forebrain ischemic injury;	Prominent expression of α -gustducin in reactive astrocytes;	Possible involvement in the glucose homeostasis in the brain after ischemia;	[43]

3.2.1 Sweet Taste Receptors in the Brain

It was first attempted to explain glucose metabolism in the brain with the called Astrocyte-Neuron Lactate Shunt hypothesis [44]: astrocytes are stimulated by glutamate received from

neurons to produce lactate through glycolysis. This lactate will then be transferred to neurons, where it can be metabolized and allow production of ATP through the Tricarboxylic Acid cycle. So far, this has been the most accepted hypothesis, but recently some pitfalls were detected in this hypothesis, as it was reported that neurons have the ability to function properly without the presence of astrocyte-derived lactate [45]. Therefore, alternative ways by which neurons can obtain and maintain an ideal amount of glucose for their own metabolism have been investigated. So far, GLUT2, ATP-sensitive potassium channel and sodium/glucose cotransporter 3 have been identified as potential candidates as glucose sensors [46], since they are located in the plasma membrane of neurons and astrocytes located in hypothalamus, brainstem and other brain regions such as the amygdala and nucleus accumbens. These brain regions are those where it is most likely to find neurons with a functional metabolism independent from the astrocyte-derived lactate.

More recent findings suggest that STRs can also play an important role in neuronal and astrocyte glucose sensing [45], consequently controlling glucose metabolism in the brain. In fact, research in animal models indicate that defects of STRs located in the hypothalamus and brainstem are associated with impairment of glucose sensing and metabolism. Also, the decrease in extracellular glucose levels in the hypothalamus leads to the increase of expression of sweet taste receptors, that normalizes after administration of sweet molecules [46].

In particular, glucose sensing in the hypothalamus can modulate food intake, glucose homeostasis and energy expenditure, which are directly related to glucose metabolism and ATP production. Similar glucose sensing mechanisms have been observed in the pancreatic β cells, where recent evidences show that STR-mediated pathways contribute to glucose β cells. This comparison resulted in the discovery that T1R2 and T1R3 are widely expressed throughout the brain, with significantly higher expression in the hypothalamus [47].

T1R2 and T1R3 levels of expression are shown to be altered according to energy status. Furthermore, high concentrations of glucose will decrease the expression of STRs, yet these are increased during caloric restriction [47]. Sensing the energy status of the system is the key initial step of energy regulation, and consequently sweet taste receptors can be important in nutrient sensing, contributing for the referred energy regulation [47].

In the hypothalamus, glucose-sensing neurons can be in either of the following two groups: glucose-excited neurons and glucose-inhibited neurons. Glucose-excited neurons are activated with high concentrations of glucose and inhibited by low concentrations of glucose, whereas glucose-inhibited neurons are activated by low concentrations of glucose and, at high concentrations, they are inhibited. The neurotransmitters of these neurons remain controversial, in spite of last observations indicate that glucose-excited neurons are anorexigenic proopiomelanocortin neurons and glucose-inhibited neurons are mostly neuropeptide Y neurons. Also, tanycytes, specialized glial cells located at the edge of the third

ventricle, can be sensitive to high concentrations of glucose [47]. Kohno et al. [48] observed that the responses of glucose-mediated neurons are mediated by the effect of sweet taste receptors because 70% of the observed glucose-excited neurons were suppressed by the inhibition of sweet taste receptors. The same role has been reported for sweet taste receptors expressed in tanycytes [47].

In a study in the rat hippocampus with transient forebrain ischemic injury, a prominent expression of α -gustducin was observed, involved in the STRs signaling in reactive astrocytes, indicating a possible involvement of STRs in glucose homeostasis in the brain after ischemia [43]. The level of STR expression in the hippocampus seems to be also associated with obesity [42], and so the hippocampus and brainstem may be key locations for metabolic modulation.

STRs have also been shown to be expressed in the choroid plexus (CP), as there is co-expression of both subunits of the receptor in CP epithelial cells, along with other taste-related proteins, such as TRPM5 and α -gustducin. It is likely that the sweet taste pathway might be one of the mechanisms through which CP can regulate glucose homeostasis of the cerebrospinal fluid [49].

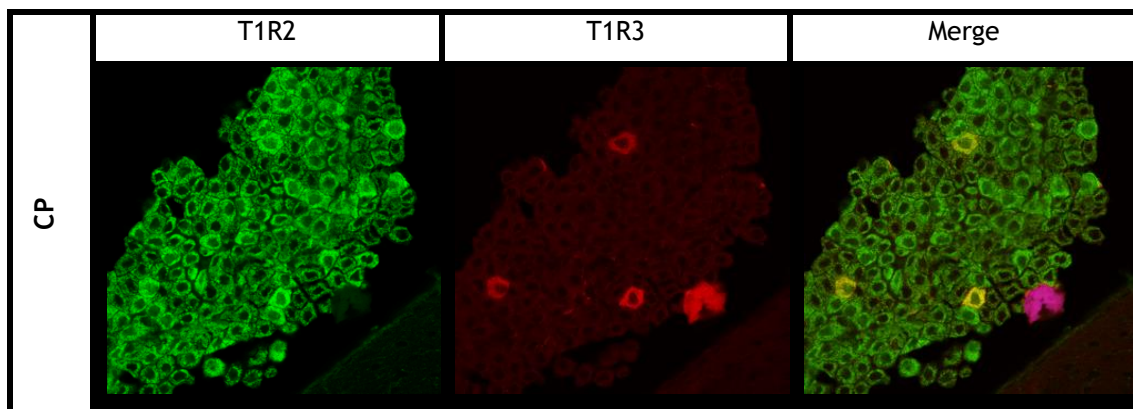


Figure 3 - T1R2 and T1R3 immunohistochemistry on mouse Choroid Plexus . Primary antibodies: rabbit anti-T1R2 1:100 and goat anti-T1R3 1:100. Secondary Antibodies: anti-rabbit AlexaFluor® 488 1:1000 and anti-goat AlexaFluor® 647 1:1000.

When it comes to the role of STRs in cancer cells, there is a prominent type of cells at which they are detected. In human gastric parietal tumour cells, STRs are present and modulate proton secretion when exposed to non-caloric sweeteners such as cyclamate and acesulfame k, consequently affecting the gastric acid environment. Moreover, it can also stimulate the release of serotonin, which can be relevant for cancer progression [41]. Apart from the mentioned case, STRs have not yet been significantly associated with cancer cells. Some papers have discussed the emergency of a better understanding of glucose metabolism in GBM as to create new paths towards innovative therapy methods. Since STRs have been shown to be both present in Central Nervous System tissue and have a role in assuring the glucose homeostasis, it is important to test whether STRs may or not be present and have an important function in maintaining the high glucose demands of tumour cells.

Aims

As it has been previously explored, STRs have been recently the target of wide research and have been discovered, not only along the entire gastrointestinal tract, but also in many other locations, one of which is the central nervous system. In some of the referred locations, there are strong indications of the STR role in glucose and metabolic homeostasis.

It is also known that GBM cells, due to their high metabolic demands, aggressiveness and chemoresistance, have specific mechanisms that will aid tumour progression. For this reason, the hypothesis underlying this study is that STRs, as glucose sensors, will have the ability to regulate GLUT1 and metabolic reprogramming in response to glucose deprivation, which is common on a tumour microenvironment.

To test this hypothesis, it is necessary to analyse if STRs are present in GBM cells and if they affect the ability of these cells to survive and proliferate in when glucose availability decreases as it occurs in tumor regions poorly irrigated. Thus, our specific objects are to:

- Compare the expression of STR subunits T1R2 and T1R3, as well as GLUT1 in GBM cells in comparison to normal human astrocytes;
- Evaluate the impact of the inhibition of STRs on GBM cell survival and migration in exposure to different concentrations of glucose.

Materials and Methods

1. Glioblastoma Cell Lines

Due to the heterogeneous nature of glioblastoma multiforme, more than one cell line was used in this work, in order to obtain a representation of different grades of GBM. The U-373MG cell line was the most proliferative and aggressive, followed by SNB19, whereas the U-87MG represents the least aggressive form of GBM. These three cell lines were used in the experiments described below.

Moreover, in *in vitro* experiments for migration and cell viability assays, GBM cells were divided into three groups: the first group was exposed to culture media containing different concentrations of glucose (0, 0.5, 1, 2.5 and 4.5 g/L); the second and third groups were also exposed to the same concentrations of glucose in the presence of 2.5 mM or 5 mM Lactisole, an inhibitor of the STR. Lactisole was firstly diluted in dimethyl sulfoxide (DMSO) at a concentration of 0.8 M. Two different vehicles of DMSO (0.3% or 0.6%) were also performed.

1.1 Cell Culture

Human malignant glioblastoma cell lines U-87MG, SNB19 and U-373MG were cultured with Dulbecco's Modified Eagle Medium (DMEM) high glucose with stable glutamine (bioWest, France) supplemented with 10% Fetal Bovine Serum (FBS, Biochrom, Berlin) and 0.1% penicillin/streptomycin (Sigma, USA), and incubated in a Culture Safe CO₂ Precision 190 incubator (LEEC, UK), at 37°C and 5% of CO₂.

1.2 Cell Passage

When confluence reached about 70-90%, cellular passages were performed to allow a continuous expansion of the cell population. For this purpose, culture medium was removed, and cells were washed with Phosphate Buffered Saline (PBS) solution 1x. After the removal of PBS 1x, trypsin-EDTA 0.25% was added in a volume that ensures the complete coverage of the cells, until cell the layer was dispersed (usually 5 minutes). Occasionally, it was necessary to incubate them for up to 5 minutes at 37°C in order to further stimulate the action of trypsin-EDTA. Then, the culture medium was added in an equal volume to the one of trypsin, cells were resuspended and collected to microcentrifuge tubes, and centrifuged for 8 minutes at 1800 rpm. The supernatant was discarded, the pellet was resuspended in 1 mL of culture medium and added to a new t-flask containing 3 mL of fresh culture medium followed by incubation at 37°C and 5% of CO₂. Cell culture medium was replaced every 2-3 days.

1.3 Cell Counting

To count cells, 10 μ L of the cell suspension were taken from and added to a microtube containing 10 μ L of trypan blue 0.4%, and 10 μ L were transferred to a Neubauer chamber (Labor Optik, Germany), in order to proceed with the counting of viable cells. The number of cells per mL were estimated through the following formulas:

$$\text{dilution factor} = \frac{\text{total volume}}{\text{volume of sample}}$$

$$\text{Cells/mL} = \frac{\text{number of viable cells}}{\text{number of quadrants}} \times \text{dilution factor} \times 10^4$$

1.4 Cell Freezing and Thawing

The freezing process of cells ensures eternalization of the cell lines. Briefly, cells were trypsinized as described in chapter 1.2, and 10% (v/v) DMSO were added to complete culture medium supplemented with 40% FBS, in order to prevent the formation of water crystals that can lead to cell lysis. Aliquots of approximately $0.5 - 1 \times 10^6$ cells were then stored at -80°C or liquid nitrogen.

Cells were thawed in a water bath at 37°C as quickly as possible, and then resuspended in culture medium, followed by centrifugation for 5 minutes at 1200 rpm. The supernatant was discarded, the pellet was gently resuspended in cultured medium, and the cell culture was performed as described above.

2. Extraction of total RNA

Total RNA extraction from the three different GBM cell lines (U-87MG, SNB19 and U-373MG) and from normal human astrocytes (HA) was performed in order to confirm the expression of the STR subunits T1R2 and T1R3 in these cells. Due to RNA's high temperature sensitivity, the entire extraction procedure was performed on ice. Moreover, since RNA can also be easily degraded by ribonucleases (RNases), strong denaturing agents were used to provoke cell lysis and further inactivate RNases present within the cell, along with diethylpyrocarbonate (DEPC) water, which was also used for the same reason.

2.1 Extraction

For the extraction, TripleXtractor reagent (GRiSP, Portugal) was added to each set of cells, at a proportion of 1 mL per 10 cm² of cells. The cells were then homogenized to allow disruption of cellular membranes, and incubated for 5 minutes at room temperature to ensure complete degradation of nucleoprotein complexes. Chloroform was then added at a proportion of 200 μ L/mL of TripleXtractor and the mixture was homogenized by inversion, followed by incubation for 10 minutes at room temperature. Cells were then centrifuged at 4°C and 12000 g for 15 minutes. From the centrifugation, each microtube content is divided in 3 phases, described in ascending order: a pink phase, constituted by protein and chloroform residues; a white interphase, containing the DNA; and a transparent aqueous phase, containing the RNA. The aqueous phase was then collected to a new microtube, to which 500 μ L isopropanol/mL TripleXtractor were added, followed by homogenization by inversion and incubation 10 minutes at room temperature, allowing RNA precipitation. Then, centrifugation for 15 minutes at 12000 g was performed, the supernatant was discarded, and the remaining pellet was washed with 500 μ L ethanol 75% diluted in DEPC water. The RNA was centrifuged at 4°C, 7500 g for 5 minutes, the supernatant was removed, and the pellet was allowed to dry, in order to remove the excess of ethanol. Finally, the RNA was rehydrated in DEPC water and stored at -80°C.

2.2 Determination and quantification of total RNA integrity

The integrity of the extracted total RNA was evaluated by agarose gel 1.5% in TAE 1x diluted in DEPC water, stained with GreenSafe (NZYTech, Portugal). Samples were prepared with 2 μ L of RNA, 8 μ L of DEPC water and 1 μ L of loading buffer, followed by electrophoresis at 80-100 V for 30 minutes and visualization onto a transilluminator UVITEC (UVITEC Cambridge, UK). RNA integrity can be confirmed through the visualization of two bands in the gel, 18S and 28S, where band 28S should have about twice the intensity of the 18S band. The total RNA was quantified using a NanoPhotometer® (Implen), and the quality and purity of the extracts was assessed through the ratio A260/A280, which gives the information of possible contamination by genomic DNA or proteins if its values are not between 1.8 and 2.1.

2.3 DNase I Treatment

For removal of possible genomic DNA contamination from total RNA samples, a DNase I treatment (Sigma-Aldrich, USA) was performed. Briefly, in a PCR tube, the equivalent of about 1 μ g of total RNA was added to 10 μ L of DEPC water, followed by the addition of 1 μ L of DNase I and 1 μ L of reaction buffer. The mixture was gently homogenized and incubated for 15 minutes at 37°C on a thermal cycler. Once the incubation had finished, 1 μ L of STOP solution was added

to each tube and the mixture was incubated at 70°C for 10 minutes. The treated total RNA samples were then used for cDNA synthesis, as described below.

3. cDNA synthesis

Complementary DNA (cDNA) was obtained by reverse transcriptase of the RNA strand. Briefly, for each RNA sample previously treated with DNase I (final volume of approximately 14 µL), a MIX1 was prepared with 2 µL of Random hexamer mix (NZYTech, Portugal) and 1 µL of DNTPs NZYMix 10 mM (NZYTech, Portugal), followed by incubation in a thermal cycler for 5 minutes at 65°C. A MIX2 containing 2 µL of RT buffer and 1 µL of NZY M-MuLV Reverse Transcriptase (NZYTech, Portugal) was added to each sample, followed by incubation in a thermal cycler at 25°C for 10 minutes, 37°C for 50 minutes, and 70°C for 15 minutes. Finally, the cDNA was stored at -20°C.

4. Reverse-transcriptase PCR

The expression of T1R2 and T1R3 in U-87MG, SNB19, U-373MG and HA was confirmed by reverse-transcriptase Polymerase Chain Reaction (RT-PCR). Forward and Reverse primers (Table 2) were designed through the Primer-BLAST tool from NCBI-NIH (www.ncbi.nlm.nih.gov/tools/primer-blast/). For a final volume of 10 µL of each reaction, 5 µL of NZYTaQ II 2x Green Master Mix (NZYTech, Portugal), 0.3 µL of Forward primer (10 µmol), 0.3 µL of Reverse primer (10 µmol), 3.2 µL of sterile water and 1 µL of cDNA were added. A tube containing 1 µL of sterile water instead of cDNA, was used as negative control, herein designated as C⁻. The reaction tubes were then placed in a thermal cycler, according to the following: 95°C for 3 minutes, 40 cycles of 94°C for 30 seconds, annealing temperature (°C) for 30 seconds and 72°C for 30 seconds, followed by final extension during 5 minutes at 72°C. For each PCR amplified products, 8 µL were visualized by 1.5% agarose gel electrophoresis in the presence of GreenSafe, as previously described in the section 2.2, in comparison to the molecular weight marker GRS Ladder 50bp (GRiSP, Portugal). After visualization on the transilluminator, the duly amplified PCR products were sent for sequencing to the company STAB VIDA (Portugal), and the sequences corresponding to the genes under study were confirmed through the Nucleotide BLAST tool from NCBI-NIH (blast.ncbi.nlm.nih.gov/Blast.cgi), by comparison with sequences from Homo sapiens database.

Table 2 - T1R2 and T1R3 Forward and Reverse primers, designed through the Primer-BLAST tool from NCBI-NIH (www.ncbi.nlm.nih.gov/tools/primer-blast/).

Gene/Accession no.	Annealing Temperature	Fragment size	Primer Sequence 5'–3'
T1R2	60°C	119 bp	Fw - CTCGGCTGTGACAAAAGCAC

NM_152232.2			Rv - CCTTGCGGGTCTGAAGAAGAT
T1R3 NM_152228.3	60°C	173 bp	Fw - GACAGAGCGCCTGAAGATCC Rv - CGATGTCGTCTGGGTTTTGC

5. Western Blot

The expression of specific proteins was performed by Western Blot, which allowed the detection of the proteins of interest T1R2 and GLUT1 on GBM cell lines and HA.

Protein extracts were obtained from HA, U-87MG, SNB19 and U-373MG cells resuspended after trypsinization, and centrifuged for 8 minutes at 1800 rpm. Then, cells were washed twice with PBS 1x, centrifuged for 7 minutes, 11000 rpm, 4°C, and the supernatant was discarded. Finally, cells were resuspended in ice-cold RIPA lysis buffer (NaCl 150 mM, NP-40 1%, sodium deoxycholate 0.5%, SDS 0.1%, Tris 50 mM), and kept on ice for at least 30 minutes. Total protein content in samples was measured using the BCA Protein Assay Kit (ThermoFisher Scientific, USA) according the manufacturer's recommendations.

Total protein (30 µg) containing β-mercaptoethanol 4% and loading buffer 1x were boiled at 95°C for 10 minutes, gently mixed and separated by SDS-PAGE using 12.5% gels and the GRS Protein Marker MultiColour (GRiSP, Portugal), first at 70 V until samples entered the resolving gel, and then at 100-120 V. Proteins were then transferred to Polyvinylidene difluoride (PVDF) membranes (GE Healthcare, USA) previously activated in methanol and equilibrated in water and transfer buffer, using the standard protocol from Trans-Blot® Turbo™ Transfer System (Bio-Rad, USA). Membranes were blocked with 5% non-fat dry milk in Tris-buffered saline (TBS) for 1 hour at room temperature, and washed 10 minutes with TBS containing 0.1% Tween (TBS-T). Then, the membranes were incubated overnight with primary antibodies rabbit anti-T1R2 (1:250, SantaCruz Biotechnology, USA) and rabbit anti-GLUT1 (1:250, SantaCruz Biotechnology, USA) diluted in TBS-T. Membranes were washed for 45 minutes in TBS-T, at room temperature, with replacement of washing solution each 15 minutes, and incubated with HRP-conjugated anti-rabbit (1:30000, ThermoFisher Scientific, USA) for 1 hour at room temperature. The washing process was repeated as described before, and antibody binding was detected using the Immobilon™ Western Chemiluminescent HRP Substrate (Millipore, USA) according to the manufacturer's instructions. Images of blots were captured with the ChemiDoc MP Imaging system (Bio-Rad, USA), and densitometry of T1R2 bands was carried out using the software ImageLab™ (Bio-Rad, USA), normalized against β-Actin. For this purpose, membranes were washed with TBS-T following detection, and incubated with primary antibody mouse anti-β-Actin (1:20000, Sigma-Aldrich, USA) for 1h30 at room temperature, followed by incubation for 1h with HRP-conjugated anti-mouse (1:40000, SantaCruz Biotechnology, USA). The washing and detection processes were performed as described above.

6. Immunocytochemistry

Immunocytochemistry was used to analyse the presence and cellular location of both STR subunits T1R2 and T1R3, as well as GLUT1, in the three GBM cell lines (U-87MG, SNB19 and U-373MG).

Briefly, cells were grown on cover glass, as described in section 1.1, until reach 60-70% confluency. Then, the culture medium was discarded, followed by washing with PBS 1x. Paraformaldehyde (PFA) 4% was added to the cells for 10 minutes for fixation, and cells were washed again thrice with PBS 1x. A blocking solution containing Bovine Serum Albumin (BSA) 3% and Triton X-100 0.2% diluted in PBS 1x was added, followed by incubation for 1 hour at room temperature. After that, cells were washed thrice with PBS 1x containing Tween-20 0.01% (PBS-T 0.01%), and incubated overnight at 4°C with primary antibodies rabbit anti-T1R2, goat anti-T1R3 and rabbit anti-GLUT1 diluted 1:100 in blocking solution. After the incubation with the primary antibodies, cells were washed several times with PBS-T, and incubated with the respective secondary antibodies anti-rabbit AlexaFluor® 488 or anti-goat AlexaFluor® 647 (1:1000 in blocking solution, ThermoFisher Scientific, USA) for 1 hour at room temperature. For T1R2 and T1R3 colocalization, was used a secondary antibody AlexaFluor® 488 biotinylated (1:800 in blocking solution, ThermoFisher Scientific, USA) for 1 hour at room temperature, followed by incubation with streptavidin (1:800) during an hour. Finally, cell nuclei were stained with Hoechst 33342 (1:1000 in PBS-T) for 10 minutes, after three washes with PBS-T, mounted on a slide with Dako Mounting Medium (Dako Agilent, USA), and visualized under a confocal microscope LSM 710 (Zeiss, Germany).

7. Migration Assay

Migration assays were performed to evaluate the cells capacity to migrate and proliferate in restricted glucose medium. GBM cell lines were cultured on a 24-well plate until reaching 90-100% confluency. Then, a scratch was created by scraping a straight line with a P200 micropipette tip. The debris were removed, and the edge of the scratch was smoothed by washing the cells once with culture medium. The FBS-free culture medium with different glucose concentrations was added to each well, in the presence or absence of lactisole, as described in section 1. To obtain the same field during the image acquisition, markings were created to be used as reference points close to the scratch [56]. After that, plates were photographed with an Olympus SP-500 UZ digital camera under an Olympus CX41 inverted light microscope at 0, 24, 48 and 72 hours after stimuli for posterior quantitative analysis. For each image, distances between one side of scratch and the other were measured at certain intervals (mm) using Fiji software [50], by comparing the images from time 0 to the last time point. Measurements taken at 0 hours from each picture were considered as the ground state.

Measurements taken at 24, 48 and 72 hours were compared individually to the ground state, at 0 hours, using the following formula:

$$\text{Migration Rate (\%)} = 100 - \left(\left(\frac{\text{Interval } 0h}{\text{Interval } x \text{ hours}} \right) \times 100 \right)$$

By using this formula, the resultant percentage will translate into the fraction of the scratch that has been filled by cells at X hours. Once cells have completely covered the scratch, the percentage would have reached 100%.

8. Cell viability assay

Cell viability was assessed in GBM cell lines by 3-(4,5-dimethylthiazol-2-yl)-2,5-diphenyltetrazolium bromide (MTT, GERBU, Germany). Briefly, $5 - 7.5 \times 10^3$ cells were seeded in 96-well plates, and the culture medium was replaced by 200 μL of serum-free medium with different glucose concentrations, in the presence or absence of lactisole. Untreated high glucose (4.5 g/L) serum-free medium was used as blank, and untreated cells were used as normalization control. MTT assays were performed after 24, 48 or 72h. Briefly, 110 μL of culture medium were discarded, and were added 10 μL of MTT solution (5 mg/mL in PBS 1x), avoiding light exposure. Ethanol 50% treated cells were used as positive control (K^+ , dead cells), of which were discarded 160 μL of culture medium, and were add 50 μL of ethanol 100%, followed by 10 μL of MTT solution. The plates were left in the incubator at 37°C, 5% CO_2 for about 20-30 minutes, allowing the formation of formazan crystals. After that time, all the culture medium was discarded and were added 100 μL of DMSO to each well. The plates were placed in an orbital shaker to dissolve crystals. Once the crystals were fully dissolved, 80 μL of each well were transferred to a new 96-well plate, which was read in a microplate absorbance spectrophotometer xMark™ (Bio-Rad, USA) at 570 nm. Data were then analysed using the Prism software (GraphPad, USA).

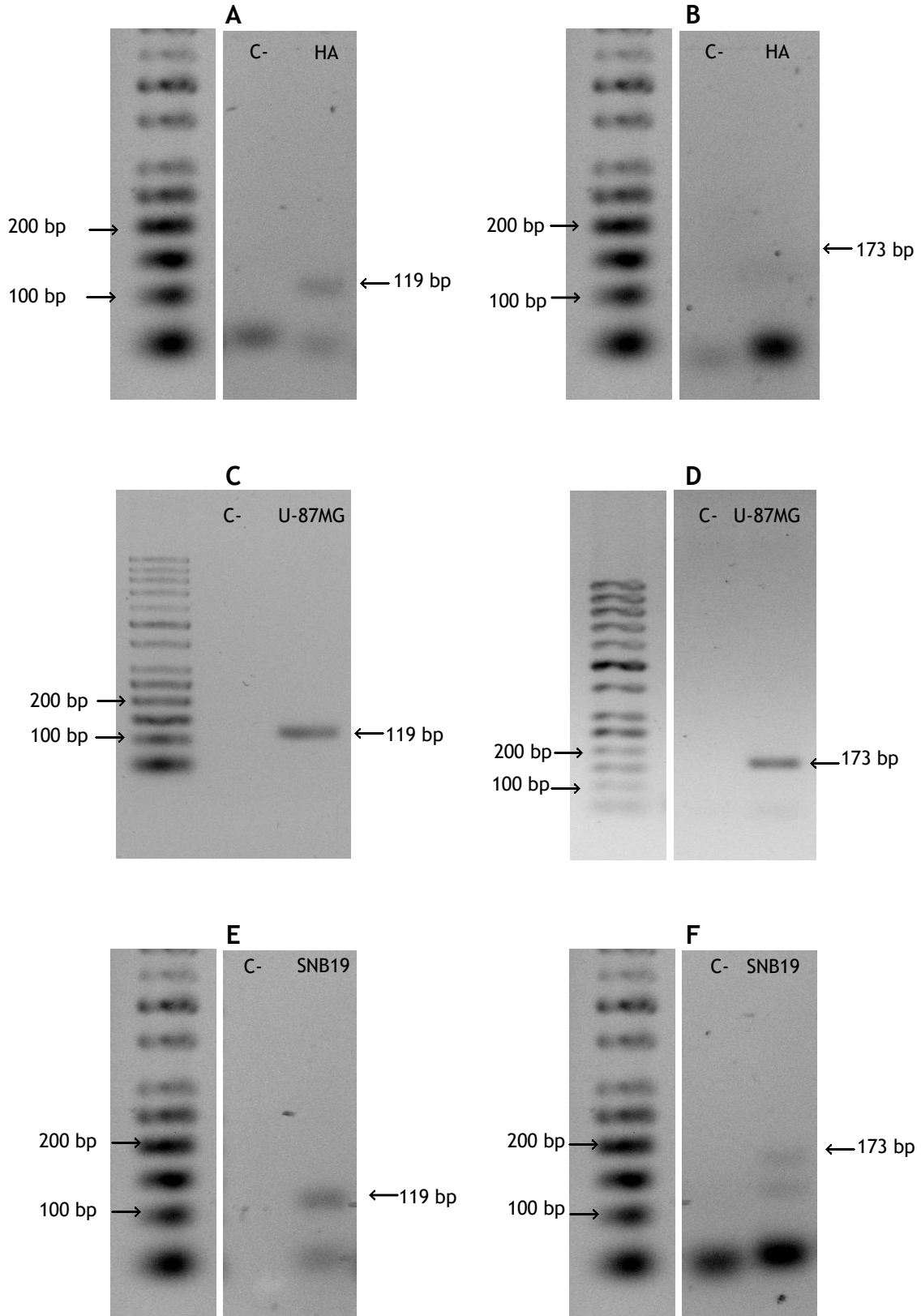
9. Statistical Analysis

Statistical analysis was carried out with the Prism software (GraphPad, USA). For the comparison of 3 or more groups, one-way ANOVA was used, followed by Dunnett's test. Data are expressed in mean \pm SEM and results were considered statistically significant when p-value < 0.05.

Results

1. Reverse Transcriptase PCR

Reverse transcriptase PCR allowed to analyse the mRNA expression of genes T1R2 and T1R3 in the studied GBM cell lines U-87MG, SNB19 and U-373MG, as well as in HA.



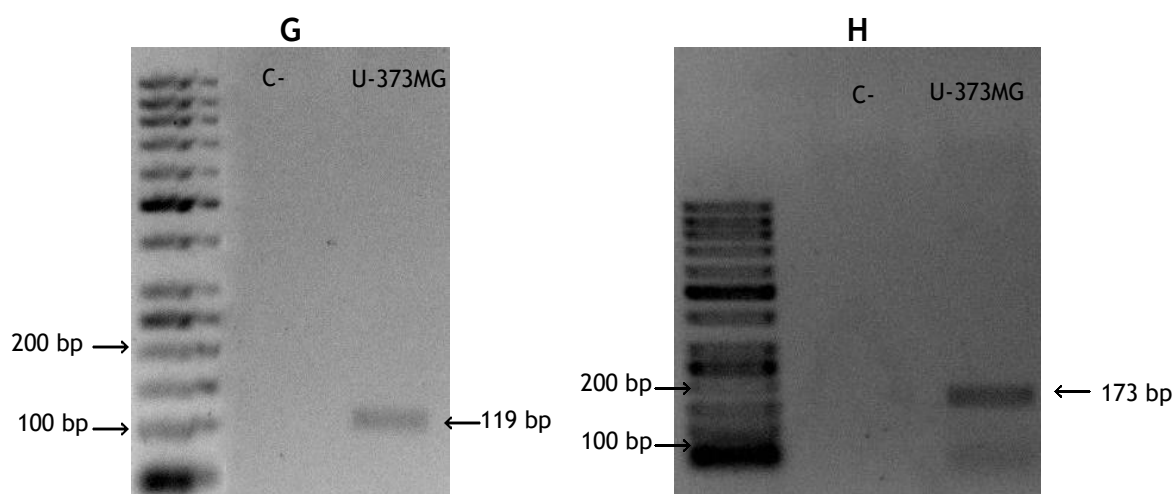


Figure 4 - Gel electrophoresis of RT-PCR products of both T1R2 and T1R3 in GBM cell lines and normal human astrocytes. (A) T1R2 expression in HA; (B) T1R3 expression in HA; (C) T1R2 expression in U-87MG; (D) T1R3 expression in U-87MG; (E) T1R2 expression in SNB19; (F) T1R3 expression in SNB19; (G) T1R2 expression in U-373MG; (H) T1R3 expression in U-373MG. Bands of T1R2 were displayed at -119 bp and bands of T1R3 were displayed at 173 bp in all tested cell lines. Alongside samples for each cDNA tested in each cell line, a negative control (C⁻) was performed.

As observed in Figure 4, there was successful amplification of genes T1R2 and T1R3 in all GBM cell lines with the predicted sizes, 119 bp and 173 bp, respectively. The same results were not observed for HA, since T1R3 was not observed or sequenced. The amplified products were sequenced by STAB VIDA (Portugal), and sequences were identified by comparison with *Homo Sapiens* sequence from NCBI-Blast database. The comparison accuracy can be verified through the given homology percentage, which was equal or above 93%, as indicated in table 3 presented below.

Table 3 - Homology percentage of T1R2 and T1R3 in all GBM cell lines and HA, when compared to *Homo Sapiens* sequence database (NCBI-Blast).

Cell Line	Receptor	Homology (%)
HA	T1R2	99
U-87MG	T1R2	99
	T1R3	93
SNB19	T1R2	100
	T1R3	100
U-373MG	T1R2	99
	T1R3	98

2. Western Blot

After confirmation of mRNA expression of STR subunits, the protein expression of T1R2 and GLUT1 was analyzed. T1R2 was chosen to be analyzed according to the availability of antibodies, as well as because it is the subunit that is not found in any other receptor and will directly indicate the presence of STRs in the cell line, contrarily to T1R3. GLUT1 was used because of its prominence as a glucose transporter in GBM cells. Both proteins were detected in the GBM cell lines U-87MG, SNB19, U-373MG and HA.

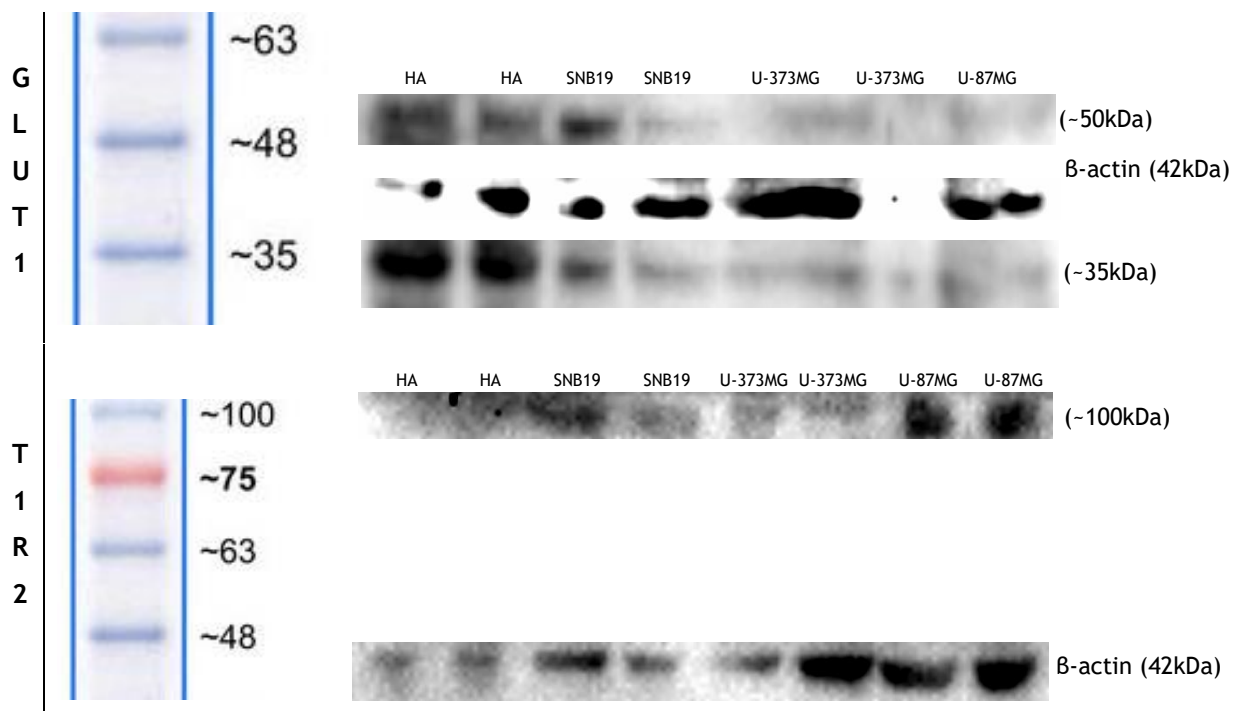


Figure 5 - Western blot of protein extracts of GBM cell lines and HA. As expected, GLUT1 were found both at ~35kDa and ~50kDa; T1R2 bands were found at ~100kDa.

In the Figure 5, it is possible to observe bands for both T1R2 and GLUT1. As expected, GLUT1 is expressed at 35 and 50 kDa, and T1R2 bands were visible for all cell lines at about 100 kDa. Densitometry of T1R2 protein bands was performed and normalized against β-actin (Figure 6). It was possible to observe that U-87MG cells have the highest T1R2 protein expression among all GBM cell lines ($p < 0.05$ relatively to SNB19 and U-373MG) and HA ($p < 0.01$).

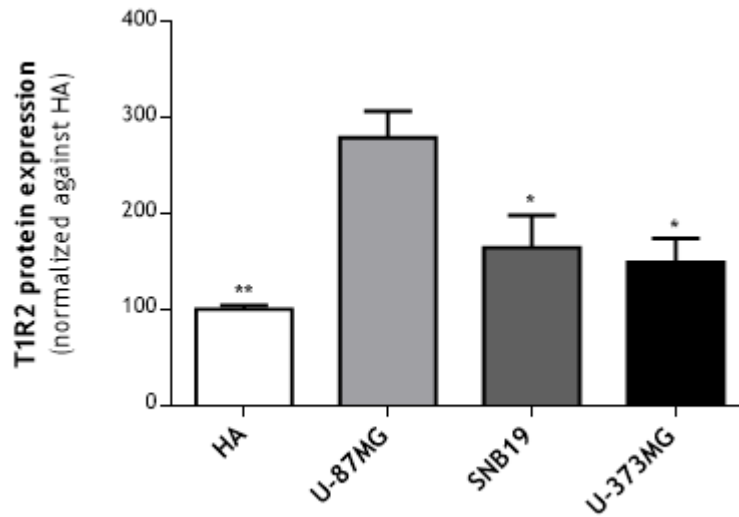
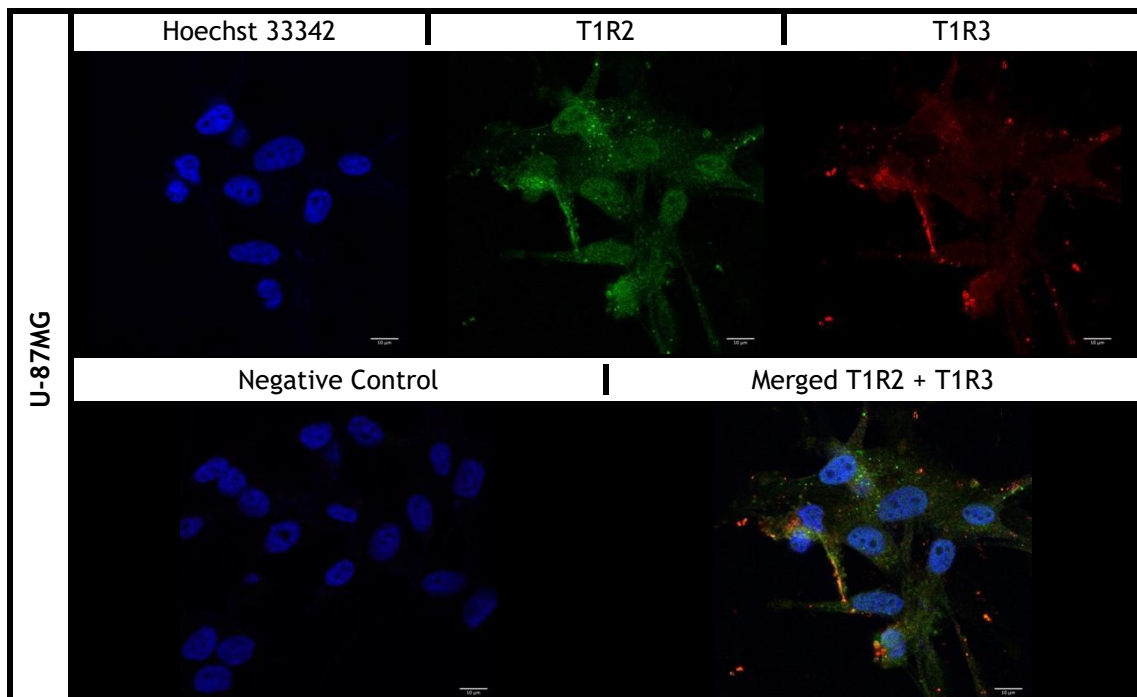


Figure 6 - Western blot quantification of T1R2 protein expression in GBM cells and HA. Densitometry of T1R2 bands was normalized against β -actin. *One-Way ANOVA* test providing the following statistical significances: * $p < 0.05$ and ** $p < 0.01$ relatively to U-87MG.

3. Immunocytochemistry

The expression and location of T1R2 and T1R3, as well as GLUT1, on GBM cell lines were analysed by immunocytochemistry.



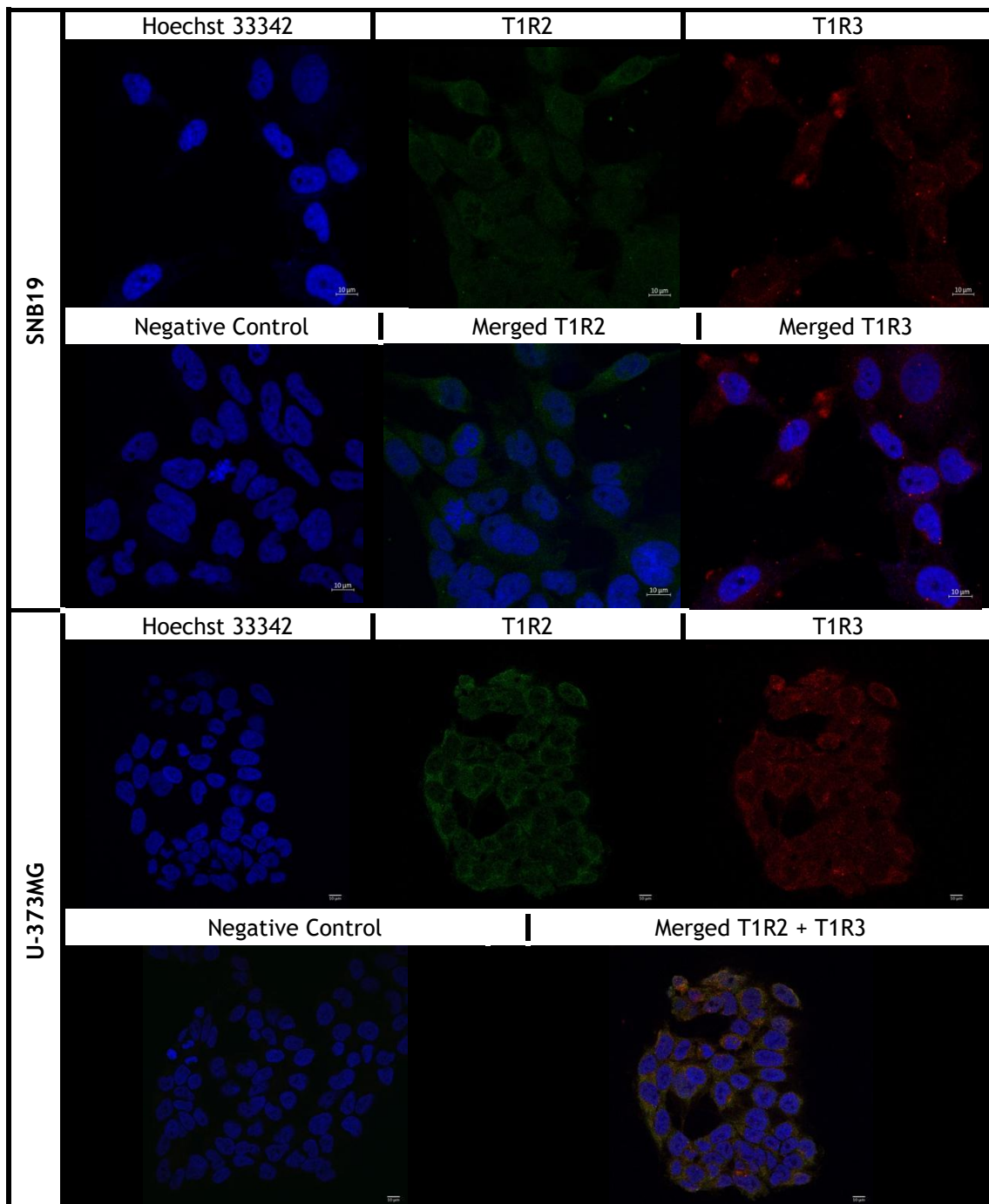


Figure 7 - Representative images for the expression of T1R2 and T1R3 in GBM cell lines U-87MG, SNB19 and U-373MG. Confocal immunofluorescence images: the AlexaFluor® 488 channel (green) represents expression of the protein of interest T1R2 and the AlexaFluor® 647 (red) channel represents the expression of the protein of interest T1R3. The Hoechst 33342 (blue) channel represents the nuclei, and the merged images are the overlap of all channels. Scale bar=10 µm.

Figure 7 shows the detection of the receptor subunits (T1R2 and T1R3) around the nucleus, particularly focused on the membrane. Concerning GLUT1, the glucose transporter most

frequently associated with GBM cells, this was detected in all GBM cell lines tested, and mostly located in the cell nucleus (Figure 8).

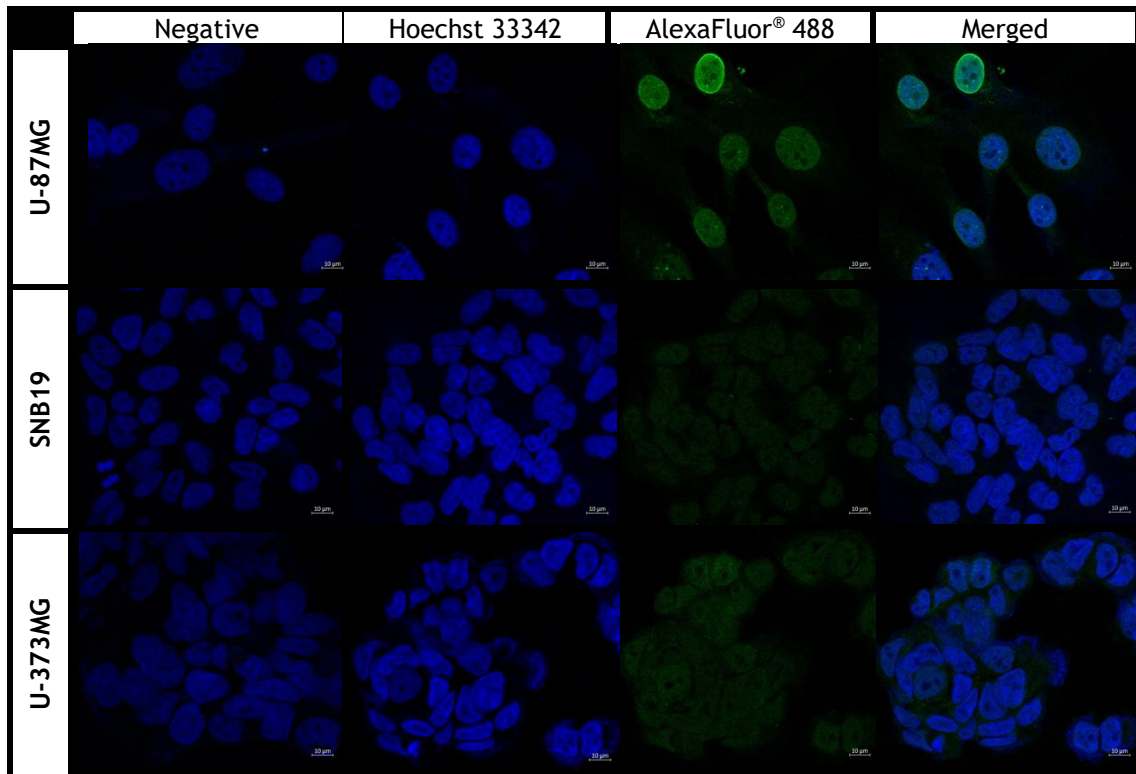
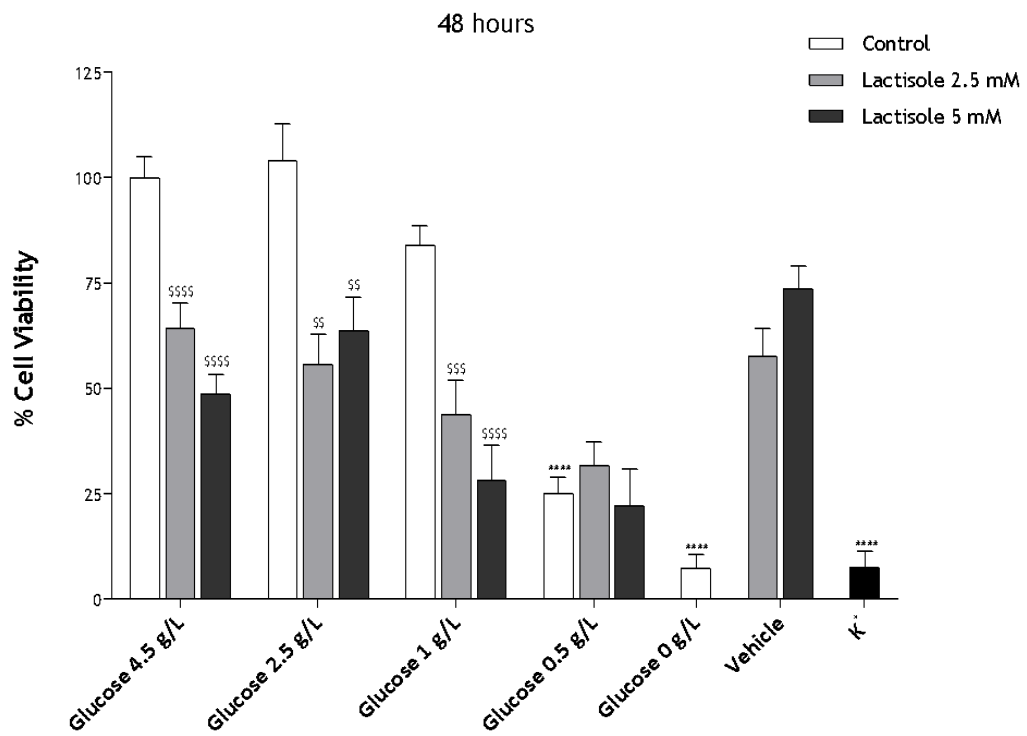
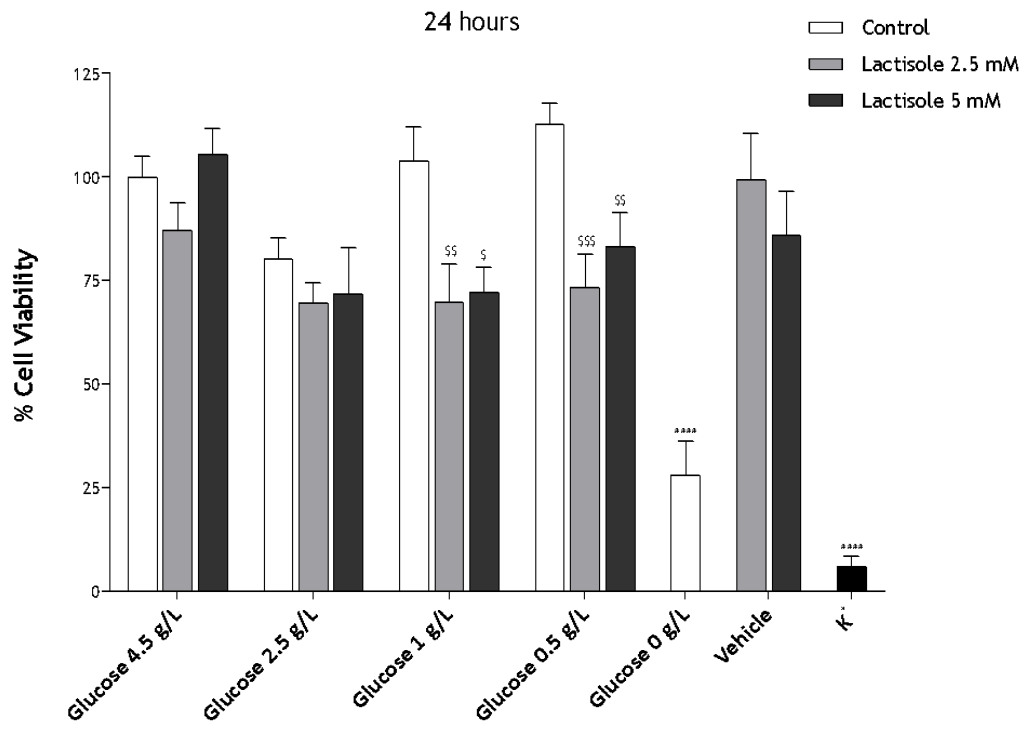


Figure 8 - Representative images for the expression of GLUT1 in GBM cell lines U-87MG, SNB19 and U-373MG. Confocal immunofluorescence images: the AlexaFluor® 488 channel (green) represents expression of the protein of interest GLUT1, the Hoechst 33342 (blue) channel represents the nuclei, and the merged images are the overlap of the two channels. Scale bar=10 μ m.

4. Cell Viability Assay

Since STRs seemed to be expressed in GBM cell lines in previous experiments, the next step was to assess their importance to cell survival. For that, cell viability assays were performed in cells cultured at different concentrations of glucose, in the presence or absence of the STR inhibitor, lactisole. Assays were performed in both SNB19 and U-373MG, since the cell line U-87MG was not available to be tested.



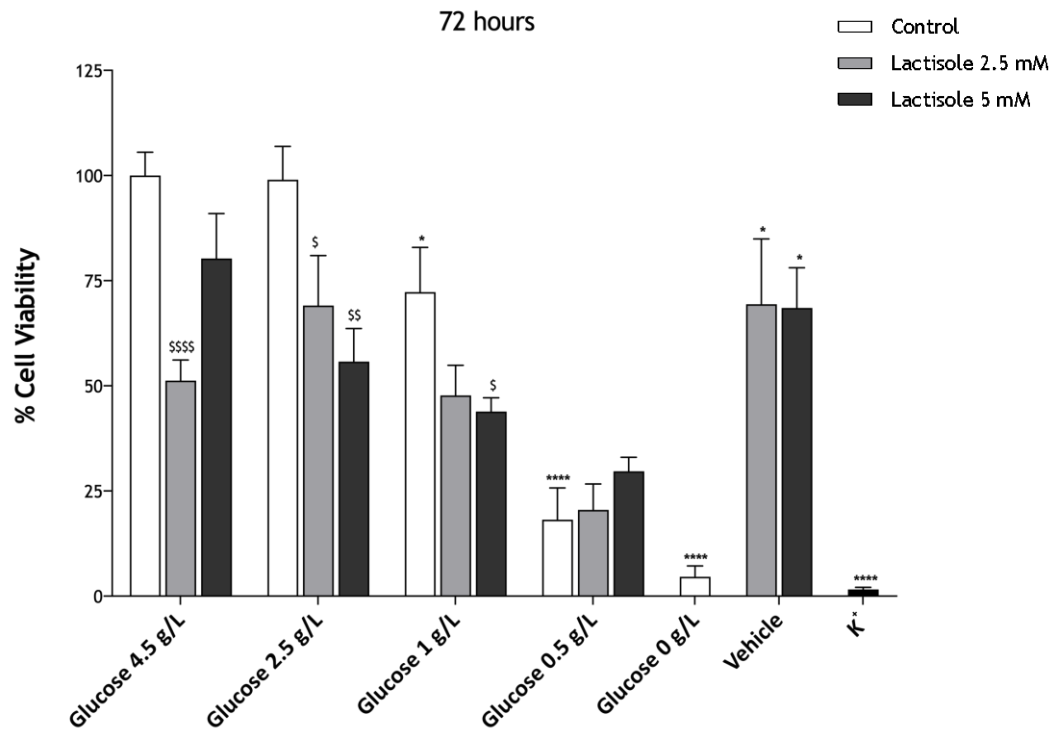
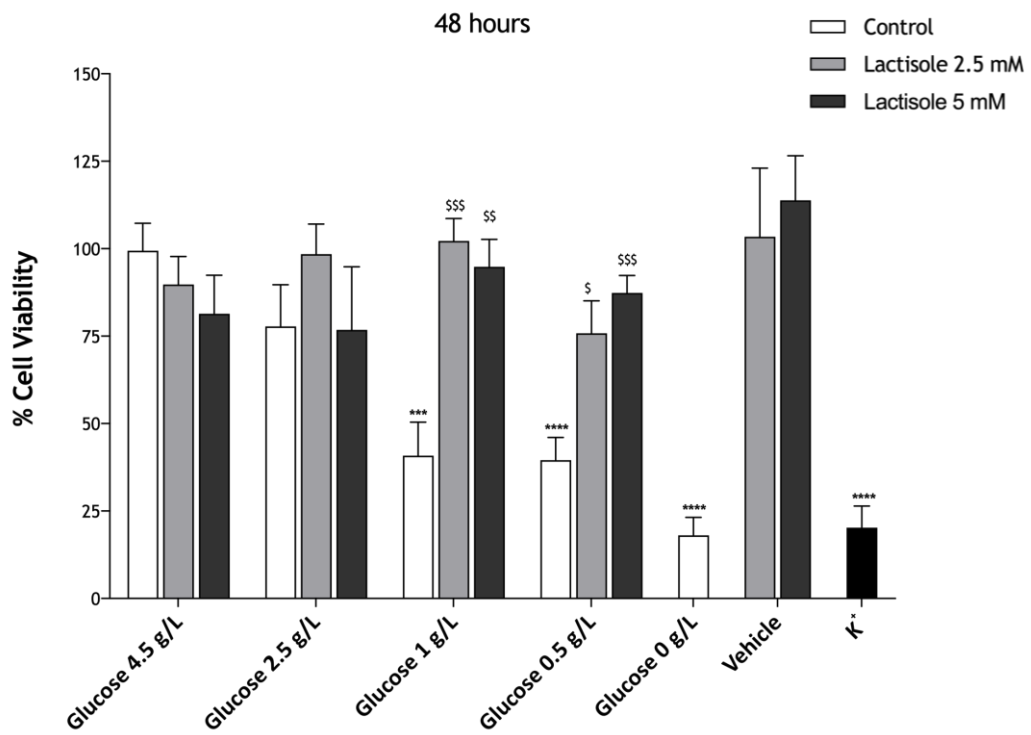
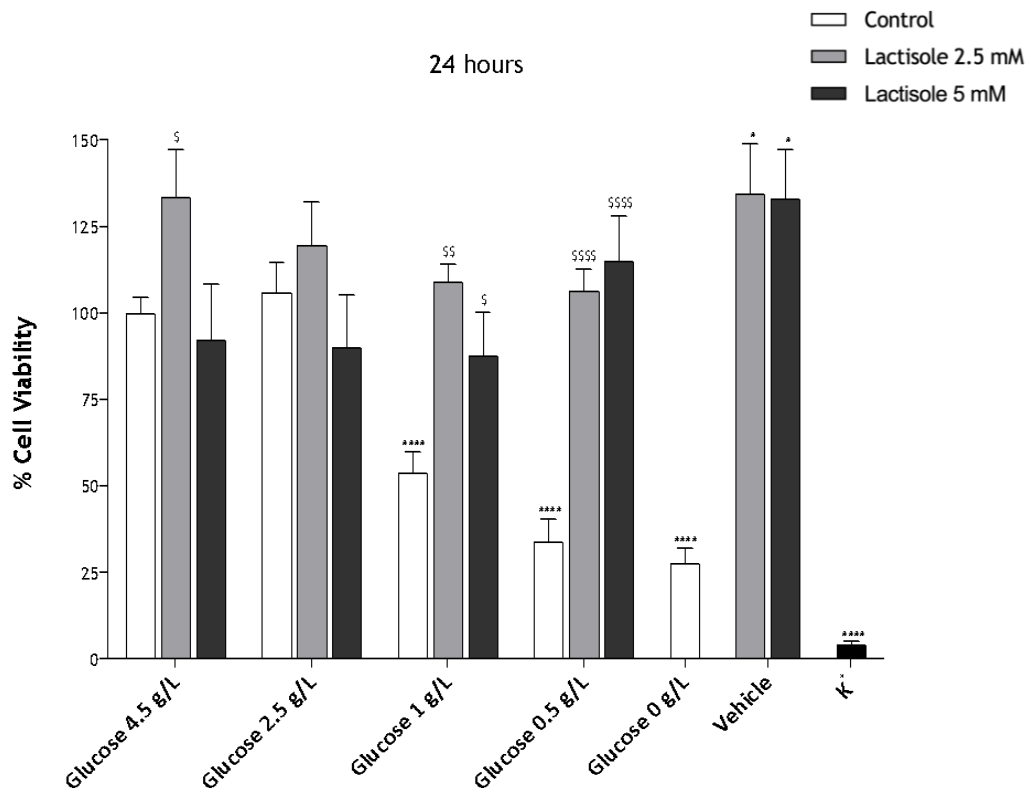


Figure 9 - Cell viability assay results for SNB19 cells at different glucose concentrations for 24, 48 and 72 hours, in the presence or absence of lactisole. K⁺: positive control; dead cells. One-Way ANOVA test providing the following statistical significances: *p<0.05 and **p<0.0001 relatively to Glucose 4.5 g/L. §p<0.05, §§p<0.01 and §§§§p<0.0001 relatively to respective glucose concentrations.**

Concerning the SNB19 cells (Figure 9), it was possible to observe that the control groups exposed to different concentrations of glucose had a similar survival rate at 24 hours, with the exception of cells with 0 g/L of glucose ($p<0.0001$). Yet, after 72 hours, there is a clear decrease of SNB19 cell survival with the decrease of as glucose concentration ($p<0.05$ for 1 g/L and $p<0.0001$ for 0.5 g/L relatively to 4.5 g/L of glucose), except for 2.5 g/L of glucose where no statistically significant differences were observed. However, in the presence of lactisole 2.5 mM, a significant negative effect in the SNB19 cells survival at 24 hours was observed in the groups of 1 g/L and 0.5 g/L of glucose ($p<0.01$ and $p<0.001$, respectively). A similar effect was observed for the lactisole 5 mM stimuli ($p<0.001$ and $p<0.01$). At 48 hours, the STR inhibition with lactisole 2.5 mM had effect in all groups from 4.5 g/L to 1 g/L ($p<0.0001$, $p<0.01$ and $p<0.001$, respectively), and inhibition with lactisole 5 mM presented similar results ($p<0.0001$ for glucose 4.5 g/L and 1 g/L, $p<0.01$ for 2.5 g/L). At 72 hours, the percentage of SNB19 cell viability decreased with STR inhibition by lactisole 2.5 mM in culture medium containing glucose concentrations of 4.5 g/L ($p<0.0001$) and 2.5 g/L ($p<0.05$). Lactisole 5 mM blocked the effect of 2.5 g/L ($p<0.01$) and 1 g/L of glucose ($p<0.05$).



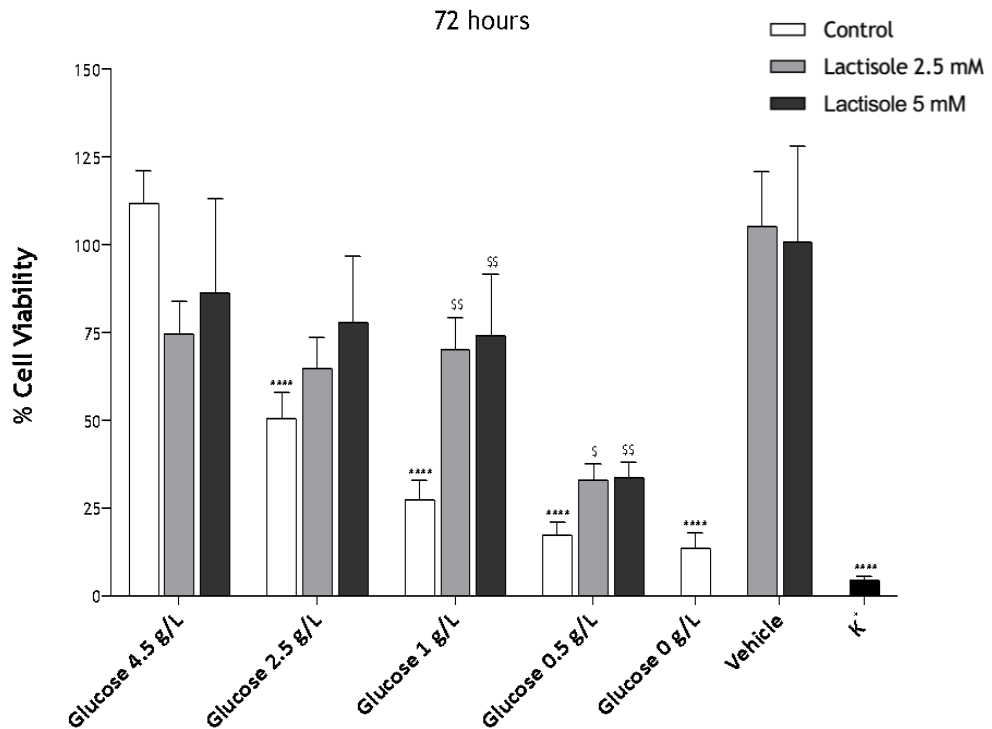


Figure 10 - Cell viability assay results for U-373MG cells at different glucose concentrations for 24, 48 and 72 hours, in the presence or absence of lactisole. K⁺: positive control; dead cells. One-Way ANOVA test providing the following statistical significances: *p<0.05, * p<0.001 and ****p<0.0001 relatively to Glucose 4.5 g/L. \$p<0.05, \$\$p<0.01, \$\$\$p<0.001 and \$\$\$\$p<0.0001 relatively to respective glucose concentrations.**

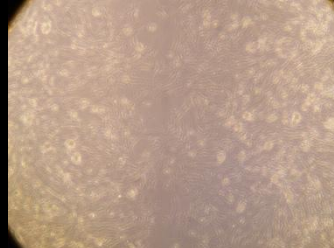
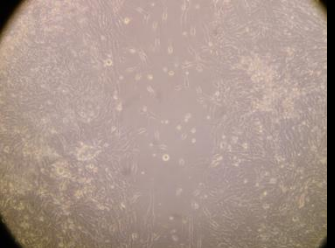

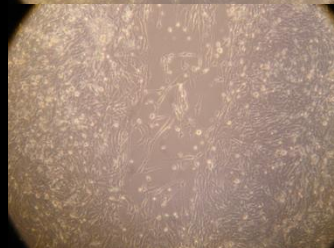
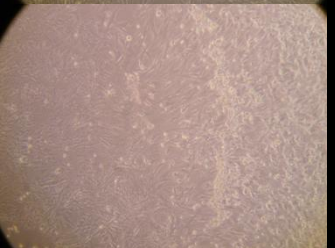

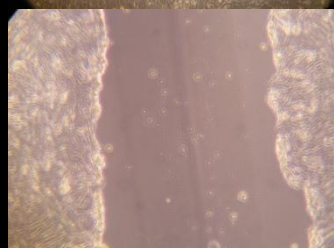
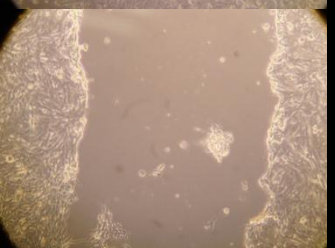
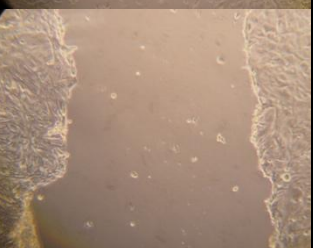
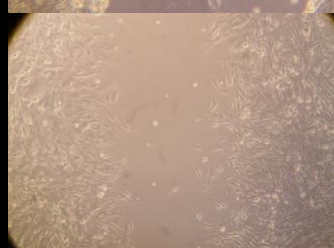
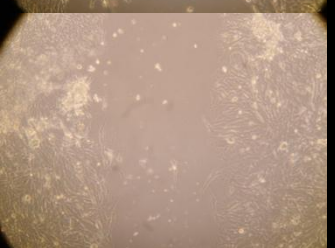
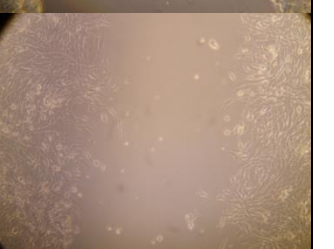
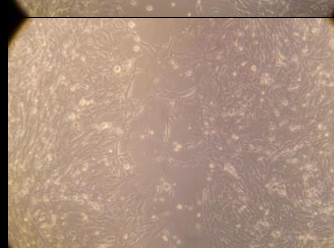



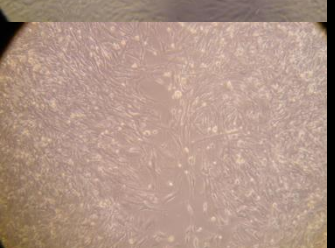

For the U373-MG cell line, results were significantly different (Figure 10). After 24 and 48 hours, only the groups glucose 1 g/L, 0.5 g/L and 0 g/L significantly decreased the percentage of viability (p<0.001 or p<0.0001). The viability of U-373MG cells incubated with culture medium containing glucose 2.5 g/L only decreased after 72 hours (p<0.0001). Relatively to the STR inhibition with lactisole 2.5 mM and 5 mM, and contrary to the results observed in SNB19 cells, the U-373MG showed a significantly higher survival, particularly visible in the groups of 0.5 and 1 g/L of glucose at 48 and 72 hours (p<0.05 for glucose 1 g/L and p<0.001 or p<0.01 for 0.5 g/L).

5. Migration Assay

It was also important not only to assess whether STRs affect GBM cell survival, but their ability to proliferate and migrate, since they are such important features of any tumour cell to promote its progression. In this assay, cells were exposed to 1, 2.5 or 4.5 g/L of glucose, as well as to 0 g/L, herein used as control, in the presence or absence of 2.5 mM or 5 mM of lactisole. Representative pictures of each group of cells are presented below (Figures 11 and 14), as well as the graphs representing the percentage of migration rate (Figures 12-13 and 15-16). The assays were performed in SNB19 and U-373MG cell lines, as U-87MG has a distinct

growth pattern because they grow in aggregates with wide space between them, instead of in a monolayer like with SNB19 and U-373MG, therefore difficulting the perception of the scratch.

		Without Lactisole	Lactisole 2.5 mM	Lactisole 5 mM
1 g/L	0h			
	24h			
	48h			
	72h			
2.5 g/L	0h			
	24h			

4.5 g/L			48h				
			72h				
			0h				
			24h				
			48h				
			72h				
			Vehicle (DMSO 0.3%)				
			Vehicle (DMSO 0.6%)				

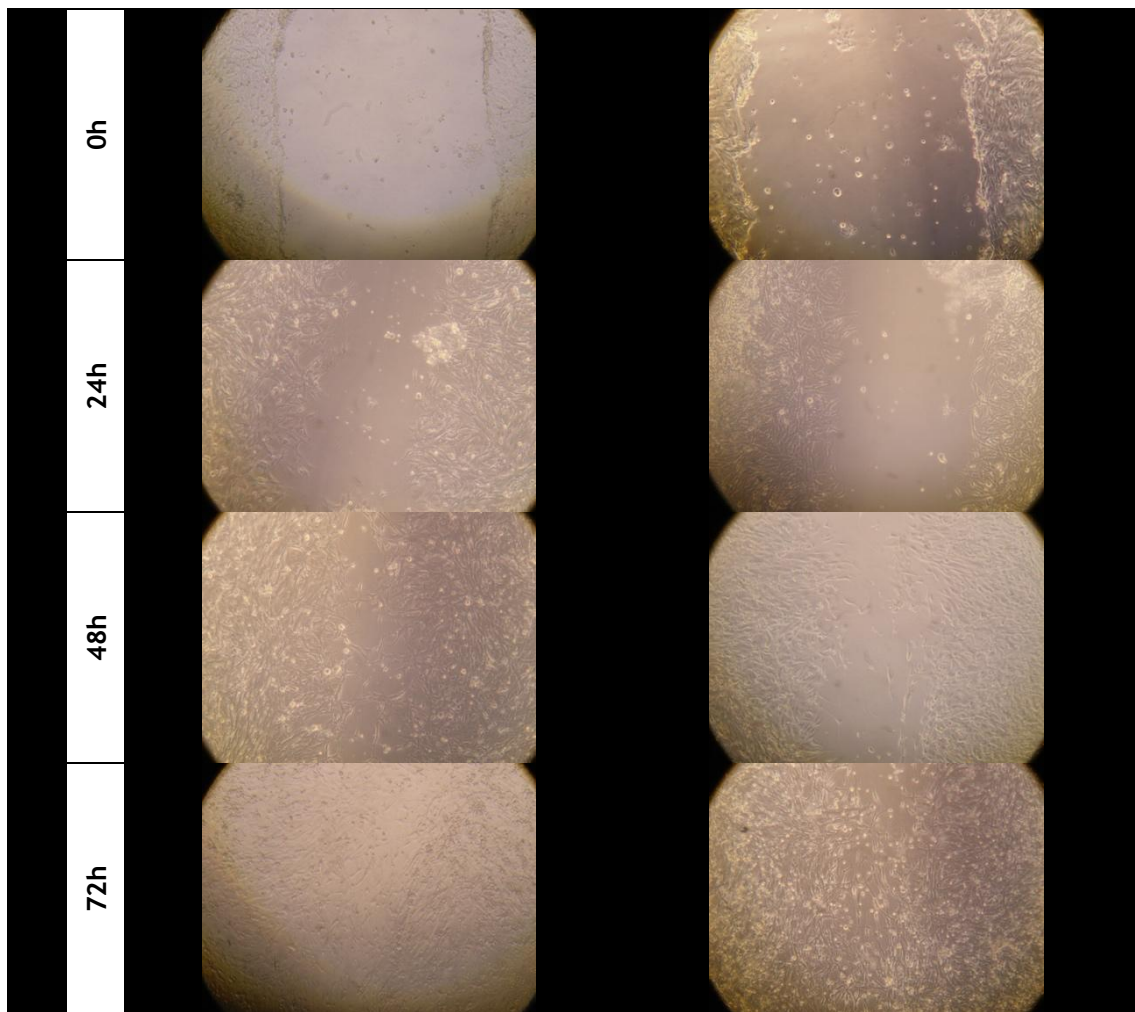
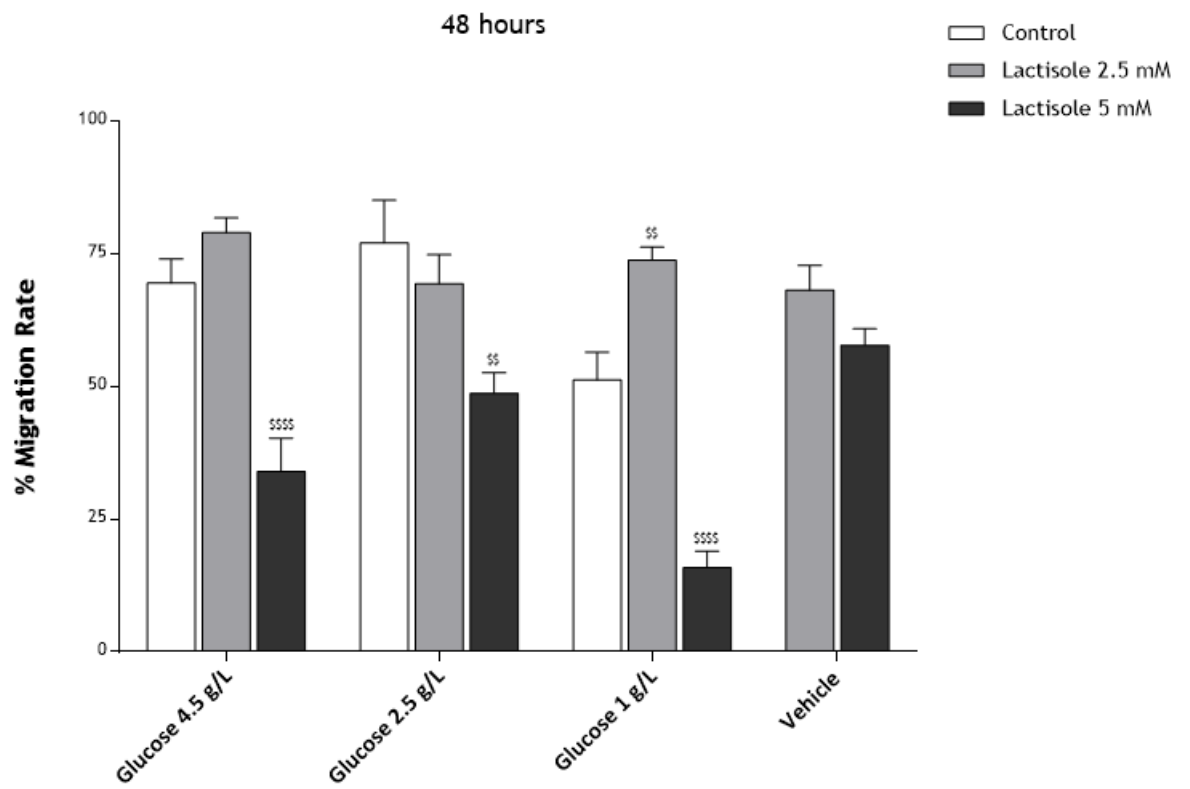
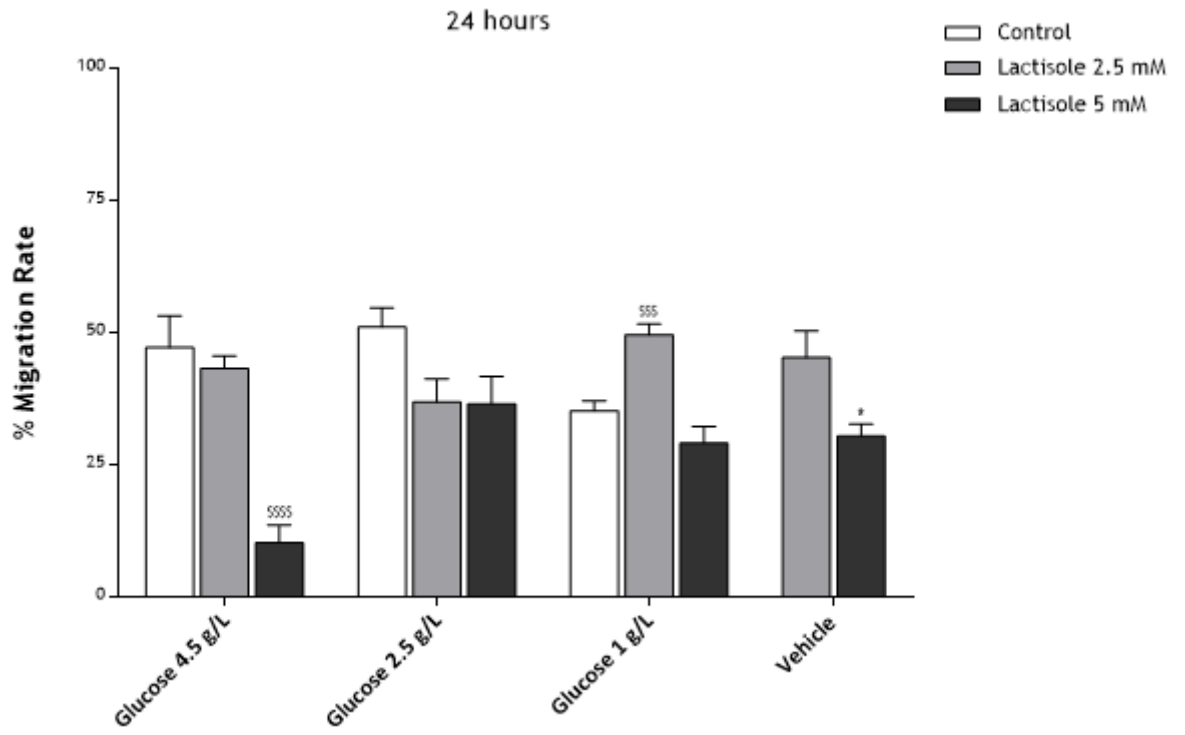


Figure 11 - SNB19 migration assay representative images at 0, 24, 48 and 72 hours after incubation with different glucose concentrations, in the presence or absence of lactisole. SNB19 cells were incubated with different concentrations of glucose (1, 2.5 and 4.5 g/L), in the presence or absence of lactisole 2.5 mM or 5 mM. Vehicles: DMSO 0.3 or 0.6%.



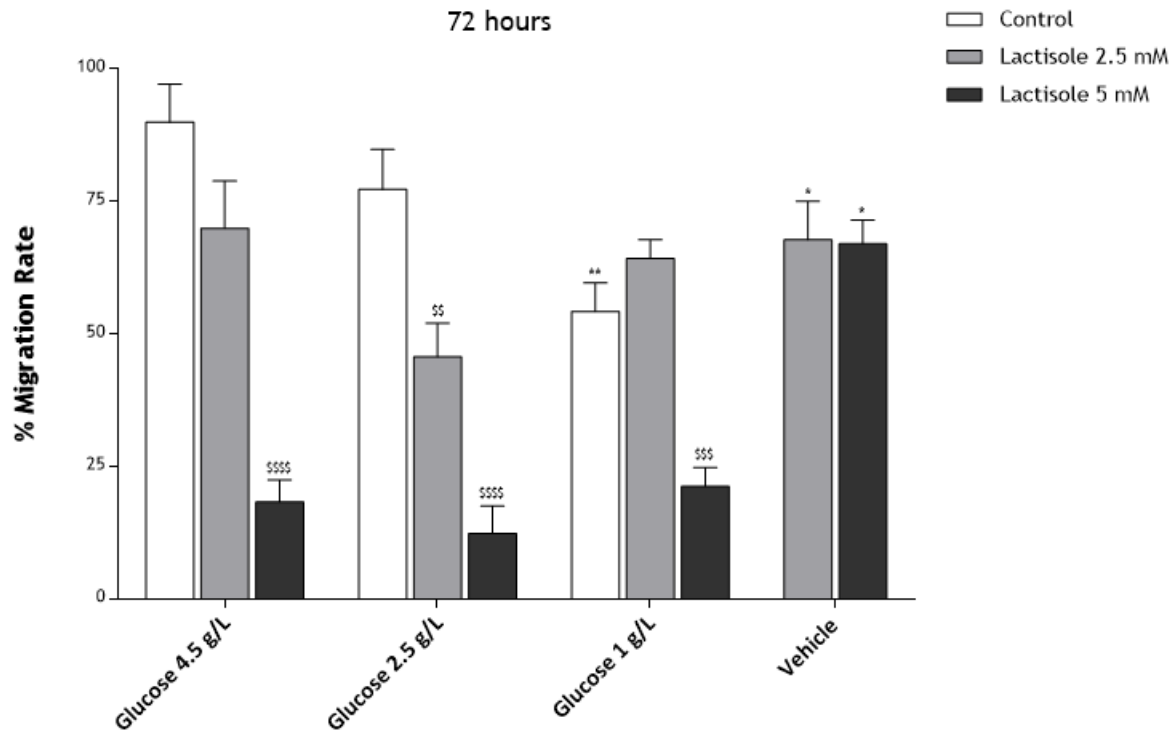


Figure 12 - Migration rate of SNB19 cells at 24, 48 and 72 hours after incubation with different glucose concentrations, in the presence or absence of lactisole. One-Way ANOVA test providing the following statistical significances: * $p < 0.05$ and ** $p < 0.01$ relatively to Glucose 4.5 g/L. $^{SS}p < 0.01$, $^{SSS}p < 0.001$ and $^{SSSS}p < 0.0001$ relatively to respective glucose concentrations.

In SNB19 cells, both from the images in figure 11 and in figures 12 and 13 of migration rate, seems that control groups migrate at a slower pace as the concentration of glucose decreased, only significant for glucose 1 g/L condition after 72 hours ($p < 0.01$). However, STR inhibition by lactisole 5 mM showed to be effective at decreasing the cells ability to proliferate and migrate, for all concentrations of glucose after 48 and 72 hours ($p < 0.001$ or $p < 0.0001$), but only for 4.5 g/L of glucose at 24 hours ($p < 0.0001$). Regarding the lactisole 2.5 mM, the STR inhibition only occurred after 72 hours for the condition of glucose 2.5 g/l ($p < 0.01$).

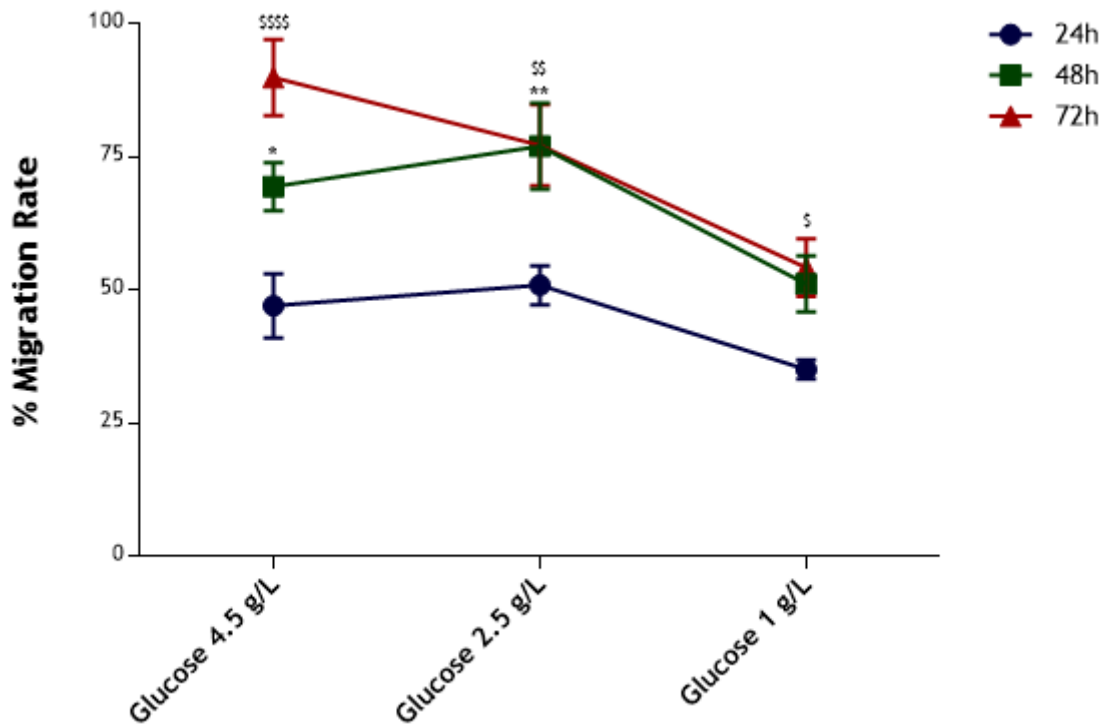
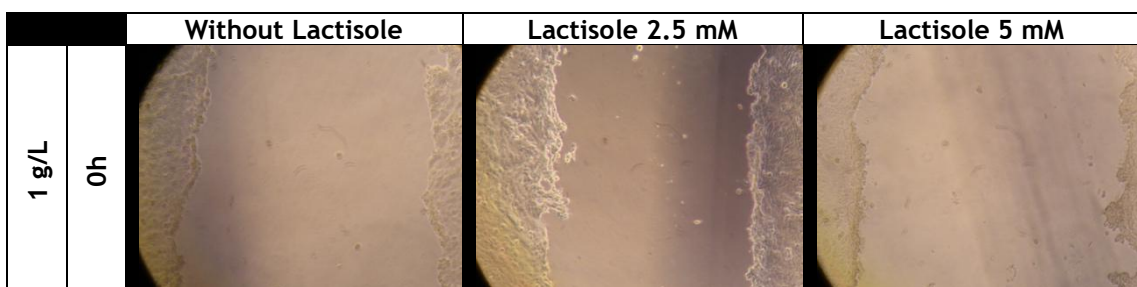
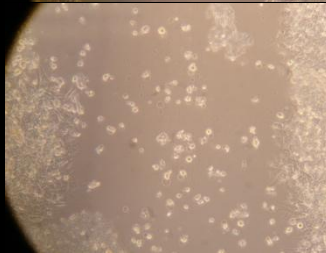
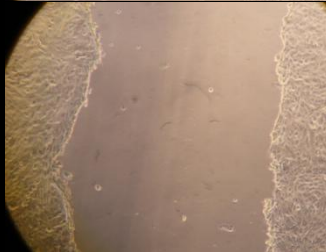


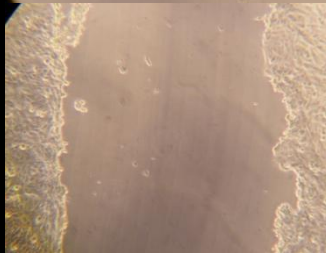

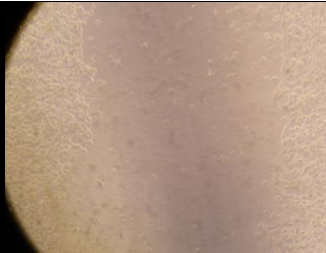

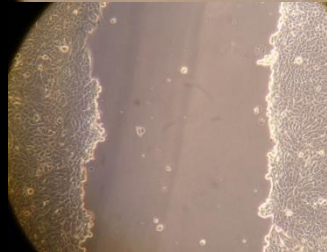
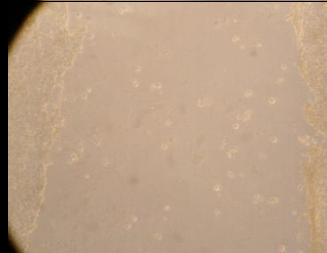
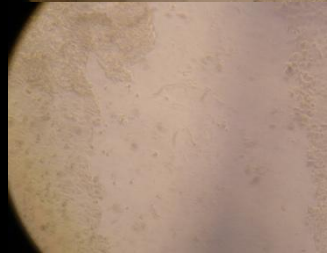


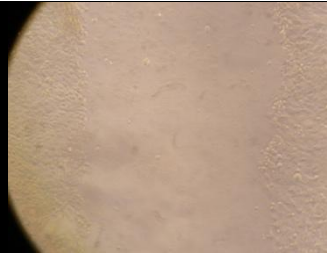

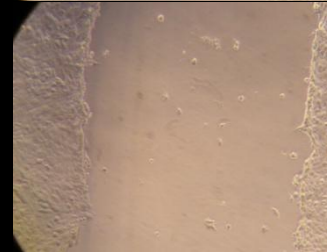

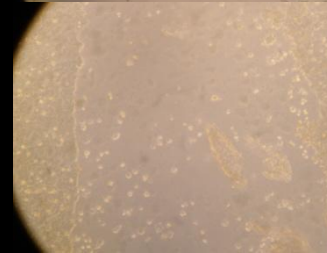


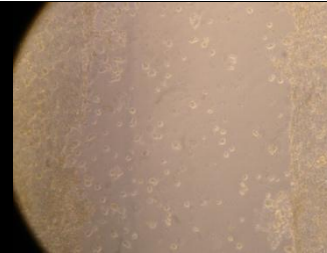


Figure 13 - Overall migration rate of SNB19 cells at 24 (●), 48 (■) and 72 (▲) hours after incubation with different glucose concentrations. One-Way ANOVA test providing the following statistical significances: * $p < 0.05$ and ** $p < 0.01$ for 48h relatively to 24h. \$ $p < 0.05$ and \$\$ $p < 0.01$ for 72h relatively to 24h.

In Figure 13 is possible to observe that, after 24 hours of SNB19 cells incubation with the different glucose concentrations, the overall migration rate was between 35-50%, and at 48 hours the migration rate increased to approximately 75% for 4.5 g/L and 2.5 g/L of glucose ($p < 0.05$ and $p < 0.01$, respectively), but no statistically significant differences were observed for glucose 1 g/L. After 72 hours, SNB19 cells exposed to 4.5 g/L of glucose were able to migrate to about 90% ($p < 0.0001$), followed by 80% migration rate for glucose 2.5 g/L condition ($p < 0.01$), and approximately 55% for SNB19 cells incubated with 1 g/L of glucose ($P < 0.05$).



4.5 g/L		2.5 g/L				
24h	0h	48h	24h	0h	48h	24h
						
						
						

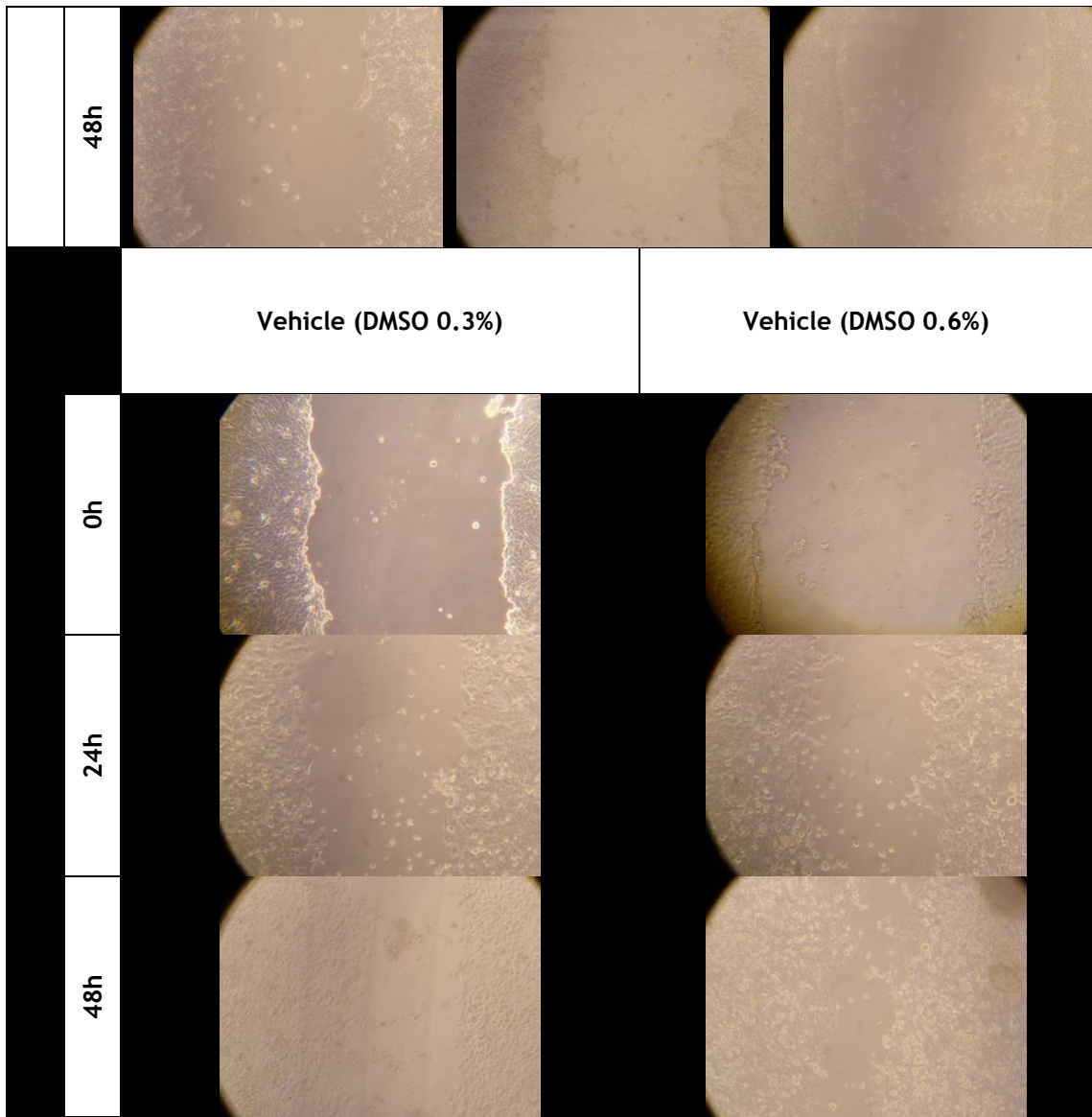


Figure 14 - U-373MG migration assay representative images at 0, 24, and 48 hours after incubation with different glucose concentrations, in the presence or absence of lactisole. U-373MG cells were incubated with different glucose concentrations (1, 2, 5 or 4.5 g/L), in the presence or absence of lactisole 2.5 mM or 5 mM. Vehicles: DMSO 0.3 or 0.6%.

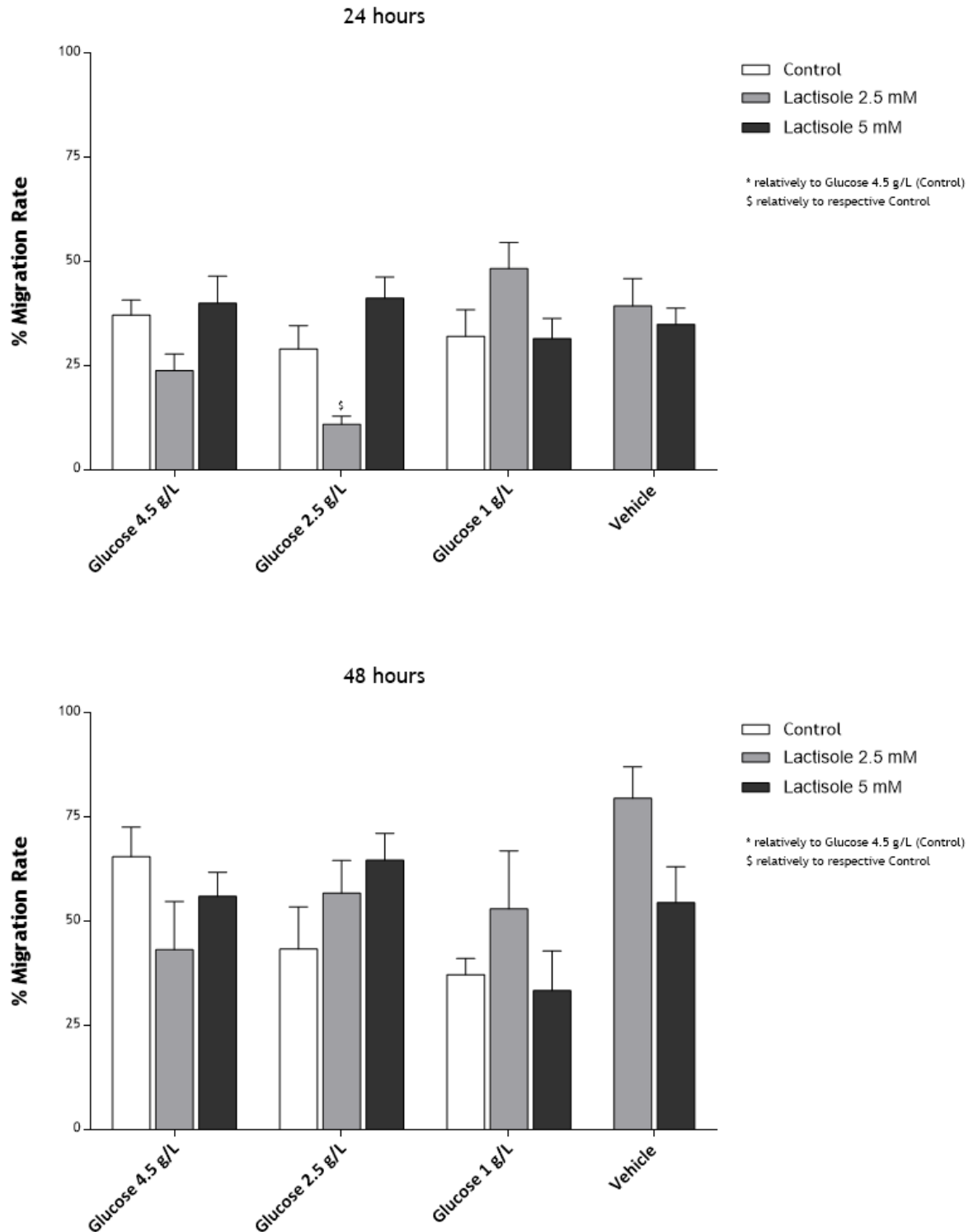


Figure 15 - Migration rate of U-373MG cells at 24 and 48 hours after incubation with different glucose concentrations, in the presence or absence of lactisole. One-Way ANOVA test providing the following statistical significances: * $p < 0.05$ and ** $p < 0.01$ relatively to Glucose 4.5 g/L. $§§p < 0.001$ and $§§§§p < 0.0001$ relatively to respective glucose concentrations.

Regarding the U-373MG cells, results were less clear (Figures 14-16). At 24 hours, only lactisole 2.5 mM inhibited the STR, triggering a decrease in migration rate of these cells ($p < 0.05$), and

by 48 hours, no significant differences were found, mainly due to the additional difficulty of performing these experiments with highly proliferative cells, like U-373MG. That's also the reason why we were unable to continue with this experiment after 48 hours, since U-373MG cells would rapidly proliferate and achieve 100% confluence, detaching from the monolayer.

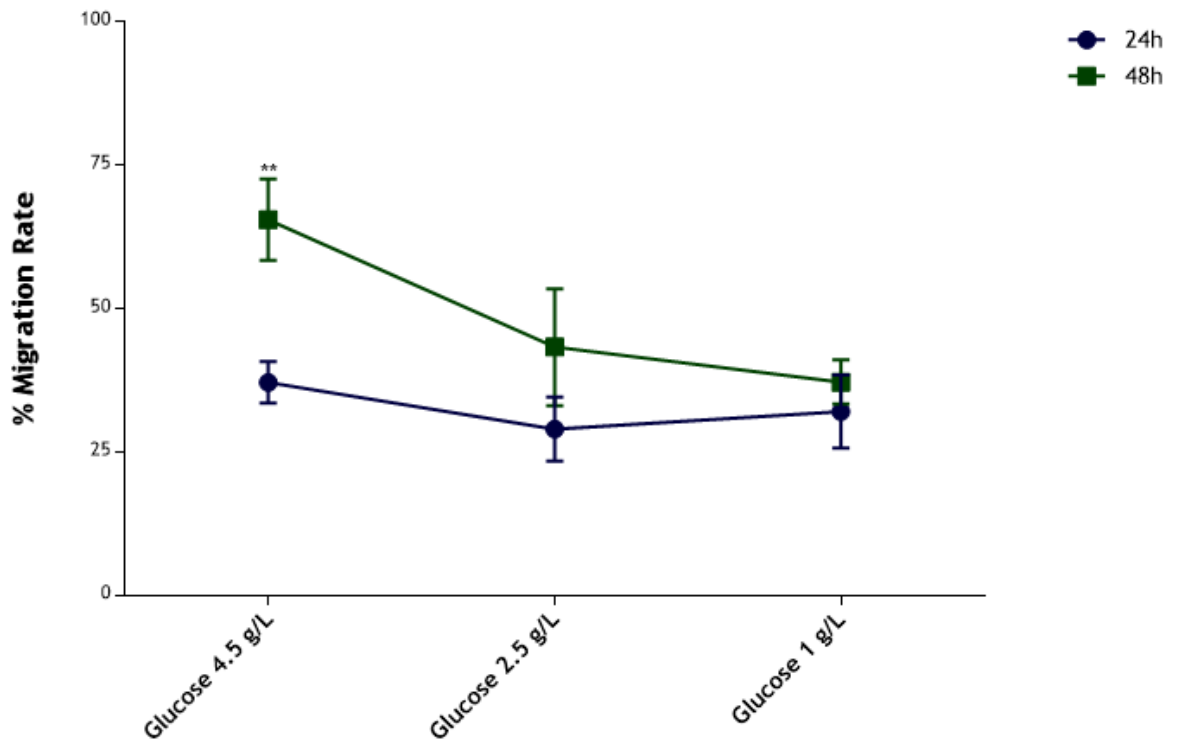


Figure 16 - Overall migration rate of U-373MG cells at 24 (●) and 48 (■) hours after incubation with different glucose concentrations. **p<0.01 for 48h relatively to 24h.

Contrary to the results observed for SNB19 cells, the overall migration rate of U-373MG only increased after 48 hours of incubation with 4.5 g/L of glucose (p<0.01) from about 35% to 65% (Figure 16). No statistically significant differences were observed for glucose 2.5 g/L and 1 g/L conditions, at 24 and 48 hours.

Discussion and Conclusion

In this study the STR was analyzed in GBM cell lines for the first time, more specifically in the GBM cell lines U-87MG, SNB19 and U-373MG. The study began with the demonstration of the presence of STR subunits T1R2 and T1R3, and GLUT1 in GBM cells using assays of Reverse Transcriptase PCR, Western Blot and Immunocytochemistry. Thus, the presence of transcribed mRNA that translates into T1R2 and T1R3 was successfully confirmed in all studied GBM cell lines, since the sequencing of the RT-PCR resultant cDNA strands confirmed their identity. However, T1R3 was not detected in normal human astrocytes. In fact, the results of RT-PCR for T1R3 in HA showed a faint band of 173 bp that could not be sequenced. The lack of intensity on the band indicates that there probably was not enough cDNA sample to be sequenced, even though the mRNA quantity used was equivalent in all tested cell lines. Thus, the expression of T1R3 in HA is either nonexistent or detrimental.

With Western Blot results, it was also possible to confirm the protein expression of T1R2 and GLUT1 in all previously considered GBM cell lines and HA. T1R2 was found within the expected size of about 100 kDa and GLUT1 was also at the expected size of about 50 kDa. Yet, strong bands represented at the size of about 35 kDa for GLUT1 were also observed [51]. With the detection of β -actin in the same protein samples, it was also possible to quantify the level of T1R2 protein expression in all cell lines. It was found that, although T1R2 is present in all cell lines, GBM cell lines have the highest levels of expression, with U87-MG showing higher expression than U-373MG and SNB19. The higher level of expression of T1R2 in U-87MG will likely indicate a more prevalent presence of STRs in this cell line, because the T1R2 subunit is only present on STRs, while the T1R3 is also common to the umami receptors constituted by T1R3 and T1R1 subunits [20]. A higher expression of STRs in these cells is likely to be an advantage to a tumour as it will enhance glucose sensing at the tumor microenvironment [52].

After confirming that GBM cells expressed STRs, their role in cell viability and migration/proliferation was assessed in a glucose restricted environment. For that, the effect of STR inhibition on the cells ability to survive when exposed to different concentrations of glucose was compared in the cell lines under study. On SNB19, in general, there was a decrease in the cell survival of controls with the decrease of glucose concentration. This confirms that the availability of glucose is crucial for cell survival, independently of STRs. When comparing controls to cells exposed to the STR inhibitor lactisole there was a significant difference found at 24 hours, with 0.5 g/L and 1 g/L of glucose, where STR inhibition was associated with a lower survival rate. However, these differences were not significant in higher glucose concentrations, which might indicate that STRs aid cells to sense and consequently transport more glucose to the intracellular environment, to be used in cell metabolism [52]. At higher concentrations of glucose, the same effect was not observed since cells still have abundant access to glucose to easily survive. However, the inhibition of the STR will also have an impact at higher concentrations of glucose after 48 and 72 hours, as glucose is being consumed. These data suggest that the inhibition of the STR will decrease cell survival in an environment lacking or

with glucose restriction. On U-373MG, there was a drastically different result. At 24 hours, an increase of survival when the STR was exposed to lactisole at 0.5 g/L and 1 g/L of glucose was already observed. With longer glucose restriction, those effects became more evident, while no significant differences were found in higher concentrations of glucose at any time point. U-373MG presents the difficulty of being the most aggressive, proliferative and chemoresistant cell line among all the ones studied and, for this reason, might have a different mechanism by which it responds to adverse metabolic conditions towards which further research should be done.

When the possible impact of STRs on GBM cells ability to migrate and proliferate was tested, the same cell lines were used as for the cell viability analysis, as well as the same conditions. Concentrations of 0 g/L and 0.5 g/L were not considered in this analysis since cell survival in these concentrations of glucose was very low, therefore compromising the ability to take measurements of migrations. With SNB19, there was a strong evidence of lower migration ability on cells with inhibited STRs, especially with 2.5 g/L of glucose, at 24 hours. After 48 and 72 hours, cells exposed to all considered concentrations of glucose suffered a significant impairment of migration ability when exposed to the highest concentration of lactisole, but no significant change was found with 2.5 mM of lactisole, except for 2.5 g/L of glucose condition. This might be explained by the cell density needed to perform the experiment. Confluence needed to be at almost 100%, which will result in a much bigger cell density than in the cell viability assays. Thus, a higher concentration of lactisole might result in a more effective inhibition of the receptor. Still, in agreement with the cell viability results, SNB19 cells will be more successful at migration rates without the STR inhibition and this effect is particularly noticeable with lower concentrations of glucose. As for U-373MG, the experiment could not be performed to completion because, by 72 hours, most cells would have detached and died, either by confluence at higher concentrations of glucose or for lack of glucose at lower concentrations. This effect was not observed in SNB19 because this cell line does not proliferate as rapidly as U-373MG. At 24 and 48 hours, however, U-373MG still did not present a significant difference whether exposed or not to the inhibition of lactisole, presenting the same behaviour observed in the cell viability assays. The results observed in the migration assay for SNB19 cells indicate a decrease of cell proliferation with STR inhibition. However, as viability assays also indicate a decrease in viability with STR inhibition, the agreement in results might indicate that STR inhibition might promote increase of cell death. Moreover, the event of apoptosis could be confirmed by performing an assay that would specifically detect apoptosis indicators, such as caspase-3 colorimetric assay or flow cytometry.

The discovery that STRs are present on GBM cells and may have an impact on their survival, definitely represents a new path of promising research. Knowing more about what influences GBM cell viability and their metabolism, could be of most interest to explore novel cancer therapy targets. Nevertheless, it is necessary to continue researching and deepen the

knowledge on how exactly do STRs act on GBM glucose metabolism and how extensively is it dependent on STRs. For example, it would be helpful to know whether the observed effects of diminished viability with STR inhibition are accompanied with a compromised Warburg effect measured by a decreased lactate release or with compromised hypoxia-induced angiogenesis. This data would let us know just how STRs can be important for the maintenance of a GBM tumour, which can in turn help with discovery of new methods of controlling or even receding GBM.

Bibliography

- [1] M. Martinez-Lage and F. Sahm, "Practical Implications of the Updated WHO Classification of Brain Tumors," *Semin. Neurol.*, vol. 38, no. 01, pp. 011-018, Feb. 2018.
- [2] G. Iacob and E. B. Dinca, "Current data and strategy in glioblastoma multiforme.," *J. Med. Life*, vol. 2, no. 4, pp. 386-93.
- [3] H. Ohgaki and P. Kleihues, "The Definition of Primary and Secondary Glioblastoma," *Clin. Cancer Res.*, vol. 19, no. 4, pp. 764-772, Feb. 2013.
- [4] F. Hanif, K. Muzaffar, K. Perveen, S. M. Malhi, and S. U. Simjee, "Glioblastoma Multiforme: A Review of its Epidemiology and Pathogenesis through Clinical Presentation and Treatment," *Asian Pacific J. Cancer Prev. J Cancer Prev*, vol. 18, no. 1, pp. 3-9, 2017.
- [5] G. C. Kabat, A. M. Etgen, and T. E. Rohan, "Do Steroid Hormones Play a Role in the Etiology of Glioma?," *Cancer Epidemiol. Biomarkers Prev.*, vol. 19, no. 10, pp. 2421-2427, Oct. 2010.
- [6] J. L. Fisher, J. A. Schwartzbaum, M. Wrensch, and J. L. Wiemels, "Epidemiology of Brain Tumors," *Neurol. Clin.*, vol. 25, no. 4, pp. 867-890, Nov. 2007.
- [7] M. Da Ros *et al.*, "Glioblastoma Chemoresistance: The Double Play by Microenvironment and Blood-Brain Barrier," *Int. J. Mol. Sci.*, vol. 19, no. 10, p. 2879, Sep. 2018.
- [8] G. Seano, "Targeting the perivascular niche in brain tumors," *Curr. Opin. Oncol.*, vol. 30, no. 1, pp. 54-60, Jan. 2018.
- [9] M. Bredel, "Anticancer drug resistance in primary human brain tumors.," *Brain Res. Brain Res. Rev.*, vol. 35, no. 2, pp. 161-204, Apr. 2001.
- [10] I. T. Papademetriou and T. Porter, "Promising approaches to circumvent the blood-brain barrier: progress, pitfalls and clinical prospects in brain cancer," *Ther. Deliv.*, vol. 6, no. 8, pp. 989-1016, Aug. 2015.
- [11] C. Jackson, J. Ruzevick, J. Phallen, Z. Belcaid, and M. Lim, "Challenges in Immunotherapy Presented by the Glioblastoma Multiforme Microenvironment," *Clin. Dev. Immunol.*, vol. 2011, pp. 1-20, 2011.

- [12] D. Beier, J. B. Schulz, and C. P. Beier, "Chemoresistance of glioblastoma cancer stem cells - much more complex than expected," *Mol. Cancer*, vol. 10, no. 1, p. 128, 2011.
- [13] N. C. Denko, "metabolism in the solid tumour," vol. 8, no. SePTeMBeR, 2008.
- [14] O. Warburg, "On the Origin of Cancer Cells," *Science (80-.)*, vol. 123, no. 3191, pp. 309-314, Feb. 1956.
- [15] M. G. Vander Heiden, L. C. Cantley, and C. B. Thompson, "Understanding the warburg effect: The metabolic requirements of cell proliferation," *Science (80-.)*, vol. 324, no. 5930, pp. 1029-1033, 2009.
- [16] S. Jawhari, M. H. Ratinaud, and M. Verdier, "Glioblastoma, hypoxia and autophagy: A survival-prone 'ménage-à-trois,'" *Cell Death Dis.*, vol. 7, no. 10, pp. 1-10, 2016.
- [17] N. C. Denko, "Hypoxia, HIF1 and glucose metabolism in the solid tumour," *Nat. Rev. Cancer*, vol. 8, no. 9, pp. 705-713, Sep. 2008.
- [18] C. M. Labak *et al.*, "Glucose transport: Meeting the metabolic demands of cancer, and applications in glioblastoma treatment," *Am. J. Cancer Res.*, vol. 6, no. 8, pp. 1599-1608, 2016.
- [19] B. Jiang, "Aerobic glycolysis and high level of lactate in cancer metabolism and microenvironment," *Genes Dis.*, vol. 4, no. 1, pp. 25-27, 2017.
- [20] A. A. Lee and C. Owyang, "Sugars, Sweet Taste Receptors, and Brain Responses," *Nutrients*, vol. 9, no. 653, pp. 1-13, 2017.
- [21] G. Nelson, M. A. Hoon, J. Chandrashekar, Y. Zhang, N. J. P. Ryba, and C. S. Zuker, "Mammalian Sweet Taste Receptors," *Cell*, vol. 106, pp. 381-390, 2001.
- [22] S. Janssen and I. Depoortere, "Nutrient sensing in the gut: New roads to therapeutics?," *Trends Endocrinol. Metab.*, vol. 24, no. 2, pp. 92-100, 2013.
- [23] X. Li, L. Staszewski, H. Xu, K. Durick, M. Zoller, and E. Adler, "Human receptors for sweet and umami taste," *Proc. Natl. Acad. Sci.*, vol. 99, no. 7, pp. 4692-4696, 2002.

- [24] A. A. Bachmanov *et al.*, “Genetics of Taste Receptors,” vol. 20, no. 16, pp. 2669-2683, 2016.
- [25] Y. Nakagawa *et al.*, “Sweet taste receptor expressed in pancreatic B-cells activates the calcium and cyclic AMP signaling systems and stimulates insulin secretion,” *PLoS One*, vol. 4, no. 4, 2009.
- [26] G. T. Wong, K. S. Gannon, and R. F. Margolskee, “Transduction of bitter and sweet taste by gustducin,” *Nature*, vol. 381, no. 6585, pp. 796-800, 1996.
- [27] A. Laffitte, F. Neiers, and L. Briand, “Functional roles of the sweet taste receptor in oral and extraoral tissues,” *Curr. Opin. Clin. Nutr. Metab. Care*, vol. 17, no. 4, pp. 379-385, 2014.
- [28] G. Servant, C. Tachdjian, X. Li, and D. S. Karanewsky, “The sweet taste of true synergy: Positive allosteric modulation of the human sweet taste receptor,” *Trends Pharmacol. Sci.*, vol. 32, no. 11, pp. 631-636, 2011.
- [29] M. Behrens and W. Meyerhof, “Gustatory and extragustatory functions of mammalian taste receptors,” *Physiol. Behav.*, vol. 105, no. 1, pp. 4-13, 2011.
- [30] A. Bachmanov *et al.*, “Genetics of Taste Receptors,” *Curr. Pharm. Des.*, vol. 20, no. 16, pp. 2669-2683, 2014.
- [31] K. Iwatsuki, R. Ichikawa, A. Uematsu, A. Kitamura, H. Uneyama, and K. Torii, “Detecting sweet and umami tastes in the gastrointestinal tract,” *Acta Physiol.*, vol. 204, no. 2, pp. 169-177, 2012.
- [32] I. Depoortere, “Taste receptors of the gut: Emerging roles in health and disease,” *Gut*, vol. 63, no. 1, pp. 179-190, 2014.
- [33] I. Kojima and Y. Nakagawa, “The role of the sweet taste receptor in enteroendocrine cells and pancreatic β -cells,” *Diabetes Metab. J.*, vol. 35, no. 5, pp. 451-457, 2011.
- [34] C. J. Berg and J. D. Kaunitz, “Gut chemosensing: implications for disease pathogenesis,” *F1000Research*, vol. 5, p. 2424, Sep. 2016.

- [35] J.-H. Park and D.-K. Song, "Sweet taste receptors as a tool for an amplifying pathway of glucose-stimulated insulin secretion in pancreatic B cells," *Pflügers Arch. - Eur. J. Physiol.*, vol. 471, no. 4, pp. 655-657, Apr. 2019.
- [36] R. Feng *et al.*, "Expression of sweet taste receptor and gut hormone secretion in modelled type 2 diabetes," *Gen. Comp. Endocrinol.*, vol. 252, pp. 142-149, Oct. 2017.
- [37] E. Karimian Azari *et al.*, "Inhibition of sweet chemosensory receptors alters insulin responses during glucose ingestion in healthy adults: a randomized crossover interventional study," *Am. J. Clin. Nutr.*, vol. 105, no. 4, pp. 1001-1009, Apr. 2017.
- [38] R. M. Carey, N. D. Adappa, J. N. Palmer, R. J. Lee, and N. A. Cohen, "Taste Receptors: Regulators of Sinonasal Innate Immunity," *Laryngoscope Investig. Otolaryngol.*, vol. 1, no. 4, pp. 88-95, Aug. 2016.
- [39] N. N. Patel, A. D. Workman, and N. A. Cohen, "Role of Taste Receptors as Sentinels of Innate Immunity in the Upper Airway," *J. Pathog.*, vol. 2018, pp. 1-8, Oct. 2018.
- [40] V. Triantafillou, A. D. Workman, M. A. Kohanski, and N. A. Cohen, "Taste Receptor Polymorphisms and Immune Response: A Review of Receptor Genotypic-Phenotypic Variations and Their Relevance to Chronic Rhinosinusitis," *Front. Cell. Infect. Microbiol.*, vol. 8, p. 64, Mar. 2018.
- [41] M. Zopun, B. Lieder, A.-K. Holik, J. P. Ley, J. Hans, and V. Somoza, "Noncaloric Sweeteners Induce Peripheral Serotonin Secretion via the T1R3-Dependent Pathway in Human Gastric Parietal Tumor Cells (HGT-1)," *J. Agric. Food Chem.*, vol. 66, no. 27, pp. 7044-7053, Jul. 2018.
- [42] D. Herrera Moro Chao *et al.*, "Impact of obesity on taste receptor expression in extra-oral tissues: emphasis on hypothalamus and brainstem," *Sci. Rep.*, vol. 6, no. 1, p. 29094, Sep. 2016.
- [43] Y.-J. Shin, J.-H. Park, J.-S. Choi, M.-H. Chun, Y. W. Moon, and M.-Y. Lee, "Enhanced Expression of the Sweet Taste Receptors and Alpha-gustducin in Reactive Astrocytes of the Rat Hippocampus Following Ischemic Injury," *Neurochem. Res.*, vol. 35, no. 10, pp. 1628-1634, Oct. 2010.

- [44] L. Pellerin and P. J. Magistretti, "Glutamate uptake into astrocytes stimulates aerobic glycolysis: a mechanism coupling neuronal activity to glucose utilization.," *Proc. Natl. Acad. Sci. U. S. A.*, vol. 91, no. 22, pp. 10625-9, Oct. 1994.
- [45] H. Benford *et al.*, "A sweet taste receptor-dependent mechanism of glucosensing in hypothalamic tanycytes," *Glia*, vol. 65, no. 5, pp. 773-789, May 2017.
- [46] M. O. Welcome and N. E. Mastorakis, "Emerging Concepts in Brain Glucose Metabolic Functions: From Glucose Sensing to How the Sweet Taste of Glucose Regulates Its Own Metabolism in Astrocytes and Neurons," *NeuroMolecular Med.*, vol. 20, no. 3, pp. 281-300, Sep. 2018.
- [47] D. Kohno, "Sweet taste receptor in the hypothalamus: a potential new player in glucose sensing in the hypothalamus," *J. Physiol. Sci.*, vol. 67, no. 4, pp. 459-465, 2017.
- [48] D. Kohno, M. Koike, Y. Ninomiya, I. Kojima, T. Kitamura, and T. Yada, "Sweet Taste Receptor Serves to Activate Glucose- and Leptin-Responsive Neurons in the Hypothalamic Arcuate Nucleus and Participates in Glucose Responsiveness.," *Front. Neurosci.*, vol. 10, p. 502, 2016.
- [49] J. Tomás, C. R. A. Santos, T. Quintela, and I. Gonçalves, "'Tasting' the cerebrospinal fluid: Another function of the choroid plexus?," *Neuroscience*, vol. 320, pp. 160-171, 2016.
- [50] J. Schindelin *et al.*, "Fiji: an open-source platform for biological-image analysis," *Nat. Methods*, vol. 9, no. 7, pp. 676-682, Jul. 2012.
- [51] F. Cyt and O. Rabmab, "Product datasheet Anti-Glucose Transporter GLUT1 antibody [EPR3915]," pp. 1-13.
- [52] B. Jiang, "ScienceDirect Aerobic glycolysis and high level of lactate in cancer metabolism and microenvironment," *Genes Dis.*, vol. 4, no. 1, pp. 25-27, 2017.